People's Democratic Republic of Algeria
Ministry of Higher Education and Scientific Research

UNIVERSITY KASDI MERBAH OUARGLA

Faculty of Applied Sciences
Department of Mechanical Engineering

END OF STUDY DISSERTATION

in view to obtain a master's degree in Mechanical Engineering

Presented by:

Boussaid Ismail

Theme

Comparison study between flat-plate and cylindrical-parabolic solar collectors (Application: Solar air conditioning)

Soutenu le: 12/06/2022
Before the jury consisting of:

-	Mr. KEBDI. Z	MCB	Président	UKM Ouargla
-	Mr. ACHOURI. EL	MCB	Examinateur	UKM Ouargla
-	Mr. GUERMIT. T	MCA	Encadreur	UKM Ouargla

Academic year: 2021/2022

بسم الله الرحمن الرحيم

وقل ربي زدني علما

Appreciation

First of all, I thank Allah Almighty for the health, will, courage and patience He has given me over these years.

I would like to thank Mr. GEURMIT for his Monitoring, understanding, advice, feedback, Support and availability during Realization of this thesis.

I am very grateful to Mr. Kebdi and Mr. Achouri Who have agreed to chair the jury.

.

Dedication

I dedicate this work to:
My Father and mother
for their sacrifice and
their presence at my side and
their support throughout
my academic journey.

SUMMARY

General Introduction 01

CHAPTER I

General information about solar energy and its deposit in Algeria

I. Introduction 04

I.1 Solar radiation 04

I.1.1 Direct solar radiation 05

I.1.2 Diffuse solar radiation 06

I.1.3 Global solar radiation 07

I.2 Position parameters 08

I.2.1 Geographic Coordinate System 08

I.2.2 Horizontal Coordinate System 09

I.2.3 Equatorial Coordinate System 09

I.3 Solar deposit in Algeria 11

I.3.1 Position parameters 11

I.3.2 Average annual insolation and average solar energy received 12

CHAPTER II

Different types of solar collectors

II.1 Physical principles of the conversion of solar radiation into heat 16

II.2 Flat-plate solar collectors..... 17

II.2.1 Diagram of a Flat-plate collector 17

II.2.2 Principle of operation 17

II.2.3 Areas of use..... 18

II.2.4 Advantages and disadvantages 20

II.3 Cylindrical-parabolic solar collectors 20

II.3.1 Diagram of a Cylindrical-parabolic collector..... 20

II.3.2 Principle of operation 21

II.3.3 Areas of use..... 22

II.3.4 Advantages and disadvantages 25

CHAPTER III

Comparison between flat-plate and cylindrical-parabolic solar collectors

III. Introduction 27

III.1 Energy balance and performance 28

III.1.1 Flat-plate collectors 28

III.1.2 Cylindrical-parabolic collectors 33

III.2 Solar absorption refrigeration machine 41

III.2.1 Performance of a solar absorption refrigeration machine 42

III.3 Parameters influencing performance of solar collectors... 42

III.3.1 Methodology.....42

III.3.2 Results and discussion ... .44

III.3.2.1 Effect of ambient temperature on the performance.....44

III.3.2.2 Effect of solar irradiance on the performance.....45

III.3.2.3 Effect of mass flow on performance.....46

III.3.2.4 Effect of collector length on performance 48

III.3.2.5 Effect of absorbent plate thickness on FPC performance.....49

III.3.2.6 Effect of the tilt factor on the performance of the CPC 50

General conclusion.....51

References

Appendices

NOMENCLATURE

SYMBOLS:

TOE : Tonnes of oil equivalent	(10^9) *Kg·m^{2}·$^{s-2}$
MTOE: Mega tonnes of oil equivalent	(10^{15})*Kg·m^{2}·$^{s-2}$
KWh: kilowatt hour	(10^6)*Kg·m^{2}·$^{s-2}$
TWh : Térawatt hour	(10^6)*Kg·m^{2}·s^{-2}
MW : Megawatt	(10^6)*Kg·m^{2}·$^{s-3}$
I : Solar radiation	W/m^2
I_T : Total solar radiation	W/m^2
I_D : direct solar radiation	W/m^2
I_d : diffuse solar radiation	W/m^2
T: Temperature	°C
D_{RO} : vertical optical density of pure and dry standard atoms	-
h: Solar Angle	degree
TLT: Actual local time	s
Cj: seasonal adjustment	-
J: number of days in the year	-
DR : Scatter radiation by Raleigh dispersion	W/m^2
DB: diffuse radiation by vapor dispersion	W/m^2
KN_{LM} : influence factor of the cloud at a low and medium level	-
N_{LM} : number of low- and medium-level clouds in tenths	-
KN_H : Concentrator Temperature	-
N_H : Cirrus influence factor	-
A_n : Surface of n	m^2
Q : Heat exchange	W/m^{2}K
$T\alpha_n$: Absorption of transmittance of n	-
U_L : Heat loss coefficient	W/m^{2}k
D_n : Diameter of n	m
L : Length	m
l : Width	m
W : Tube spacing	m
h_n : Convection heat transfer coefficient of n	W/m^{2}K
e : Thickness	m
F : Collector efficiency factor	-
F' : Effectiveness of the fins	-

F_R: Heat Removal Factor	-
S: Absorbed flux S	W/m^2
$\dot{m}$: Mass flow rate	kg/s
Cp : Specific heat	kJ/kgK
v : velocity	m/s
Re : Reynolds number	-
Nu : Nusselt number	-
Pr : Prandtl number	-
V : Dynamic viscosity of n	$N\ s/m^2$
q : Heat loss rate	J/s
R_a : Rayleigh's number	-
R_a' : Modified Rayleigh number	-
L_C : Radial gap	m
C : Concentration ration	-
R_b : Tilt factor	-

GREEK:

Φ : Latitude	degree °
δ: declination angle	degree°
ω : Time angle	degree°
θ: Angle of incident	-
y : Interception Factor	-
p : Reflectivity of the concentrator surface	-
σ : Density	kg/m^3
λ_n : Thermal conductivity of n	W/m^2K
λ : Wavelength	m
ζ: Zenith distance	m
α: geographical latitude of the place of observation	degree
β: angle of the sun above the equator at the time of observation	degree
ξ : time angle of the sun	degree
τ_n : Transmittance of n	-
α_n : Absorption of n	-

ABREVIATIONS:

COP: Coefficient of performance
CPC: Cylindrical-parabolic Collectors
CSP: Concentrating solar power
DEC: declination
DHW: Domestic hot water
ECS: Electronic Control System
FPC: Flat-plate Collectors
HEX: Heat exchanger
HTF: Heat transfer fluid
IPH: Industrial process heat
NOM: National Meteorological Office
NREL: National Renewable Energy Laboratory
PV: Photovoltaic
RA: Right ascension
SARM: Solar absorption refrigeration machine
SOLPOS : Solar Position
STR: Solar thermal ratio

LIST OF FIGURES

Figure I-1: Proportion of diffuse radiation in total radiation I_T…….…….....5

Figure I-2: Irradiation of the Sun and Earth…….…..…....8

Figure I-3: The Geographic Coordinate System…….…...8

Figure I-4: The Horizontal Coordinate System …….....9

Figure I-5: The Equatorial Coordinate System…….....10

Figure I-6: solar sites in the world / map of Algeria……11

Figure I-7: Temperature distribution in Algeria……12

Figure I-8: Solar irradiation in Algeria... …….....13

Figure II-1: Diagram of an absorption refrigeration machine ……..16

Figure II-2: Diagram of a flat plate solar collector ... …….....17

Figure II-3: Illustration of thermal and optical losses in a flat plate collector…….....18

Figure II-4: Flat plate solar collector with closed loop water heater.....18

Figure II-5: Diagram of an active solar heating system... …….....19

Figure II-6: Diagram of a parabolic trough concentrator... …….…...21

Figure II-7: A solar thermal system using parabolic collectors ... …….....22

Figure II-8: Diagram of a parabolic trough water heating system... ……..23

Figure II-9: Standard industrial parabolic trough concentrator system ... ……...……...23

Figure II-10: Solar-assisted air conditioning via a domestic heating network... ……..……..24

Figure II-11: Diagram of a solar-powered MED desalination plant... ……...…25

Figure III-1: Heat flow through a flat plate solar collector...……...……..28

Figure III-2: Typical solar energy collection system...……...……...28

Figure III-3: Performance of a typical flat plate thermal collector... …….32

Figure III-4: Cross-section of the cylindrical parabolic collector... …….....33

Figure III-5: Performance of a cylindrical-parabolic solar collector... ……..40

Figure III-6: Applications of solar-absorbed refrigeration systems……41

Figure III-7: Schematic diagram of SARM……..... 42

Figure III-8: Efficiency of the FPC as a function of the ambient temperature ... ……. 44

Figure III-9: Efficiency of CPC as a function of ambient temperature ... ……. 44

Figure III-10: Efficiency of FPC according to solar irradiance……...45

Figure III-11: Efficiency of CPC according to solar irradiance ……..45

Figure III-12: Efficiency of the FPC according to the mass flow rate ṁ…….46

Figure III-13: Efficiency of the CPC according to the mass flow rate ṁ…….47

Figure III-14: Efficiency of the FPC according to the length of the collector L……..48

Figure III-15: Efficiency of the CPC according to the length of the collector L……..48

Figure III-16: Efficiency of the FPC according to the thickness of the absorbent plate e_p…...49

Figure III-17: Efficiency of CPC according to the tilt factor R_b……50

LIST OF TABLES

Table I-1: Solar potential in Algeria……12

Table III-3: Solar radiation and ambient temperature at Ouargla at 11:00……..30

Table III-1: Solar radiation in Ouargla on May 18, 2022. a 6:00 from 19:00…….37

Table III-2: Fixed values of the FPC to be used in the study……43

Table III-3: Fixed values of the CPC to be used in the study……...43

GENERAL INTRODUCTION

General Introduction:

The North African region faces a wide range of challenges, including a rapidly growing population, slower economic growth, high unemployment rates and significant environmental pressures. This leads to an increase in energy demand in developing countries. In addition, fluctuating fuel prices are a major concern faced by many countries that rely heavily on conventional electricity generation to meet charging demand. Therefore, the need to use alternative resources, such as renewable energy, is crucial to mitigate dependence on fossil fuels, while ensuring a reduction in carbon dioxide emissions [1]. Algeria, which is the country with the largest area in Africa, has experienced rapid growth in energy demand over the past decade due to the significant increase in the residential, commercial and industrial sectors. Currently, the hydrocarbon-rich country is heavily dependent on fossil fuels for electricity generation, with renewables having only a small contribution to the country's energy mix [2].

In Algeria, energy consumption at the national level is increasing year by year due to demographic and urban development, in addition to the constantly increasing economic development. As for resources, based mainly on oil and natural gas, they are not unlimited and are slowly depleting [3]. National commercial energy consumption increased from TOE 6 million (MTOE) in 1970 to just under 40 MTOE in 2005 [3], tripling unit consumption in 30 years. Electricity production in Algeria was 25.8 billion kWh in 2002 and 30.06 billion kWh in 2005 and the country's consumption is between 25 and 30 TWh/year. In a context of economic recovery, energy demand doubled in 2020, reaching 59 MTOE. With the exception of a slight slowdown in 2016-2017, demand grew steadily by 5% per year on average over the period 2010-2019, due to the increase in energy uses and economic activities [2].

Algeria also has one of the largest solar deposits in the world, with a very high annual average of insolation. It is also the largest in the entire Mediterranean basin with considerable average solar energy received in the Sahara of Algeria [4].

Solar energy is a clean and abundant source of energy that is characterized by an absence of pollution. Therefore, it appears that solar energy can provide real solutions to the various problems that currently arise with regard to climate change, energy crises.

Solar collectors are used to collect energy from the sun, absorbing solar radiation and converting it into heat or electricity. The type of material and coating of a solar collector are used to maximize the absorption of solar energy.

For solar collectors to work at high temperatures, it is necessary to increase the incident optical flux, this could be achieved by focusing the solar radiation, this operation can be carried out with the help of collectors such as flat plate and Cylindrical-parabolic collectors [5].

Cylindrical-parabolic collectors usually have a reflective surface in cylindrical-parabolic form intended to concentrate solar energy on an absorbent surface, which allows a sharp increase in heat.

On the other hand, flat plate collectors use a plate to absorb heat and Supply to a fluid that flows through pipes that is then transferred or stored.

The objective of our work is to make a comparative study of two solar collectors, the flat solar collector and the cylindrical-parabolic solar concentrator for the application of solar air conditioning in the region South-East of Algeria specifically the state of Ouargla.

This dissertation has three chapters beginning with a general introduction and ending with a general conclusion:

➔ The first chapter is devoted to generalities on solar energy and its deposit in Algeria.
➔ The second chapter is devoted to the principles of the convergence of solar radiation into heat and different types of solar collectors
➔ The third chapter is devoted to the comparison between the two collectors and the influence of the different parameters on the efficiency of the flat-plate solar collector and the cylindrical-parabolic solar concentrator.

Chapter I

General information on Solar energy and Its deposit in Algeria

I- Introduction:

Solar power generation involves the use of solar energy (radiation) to provide hot water via solar thermal systems or electricity via solar photovoltaic (PV) and concentrated solar power (CSP) systems, these technologies are technically well proven with many systems installed around the world in recent decades Solar Photovoltaic. (PV) systems convert solar energy directly into electricity. The cornerstone of a photovoltaic system is the photovoltaic cell, which is a semiconductor device that converts solar energy into direct current electricity.

Photovoltaic systems are very modular, they can be connected to each other to provide power ranging from a few MW to tens of MW [6].

Photovoltaic conversion is based on the photovoltaic effect, i.e., on the conversion of solar energy from the sun into electrical energy. To perform this conversion, devices called solar cells are used, consisting of semiconductor materials in which a constant electric field has been artificially created.

The process of thermal conversion of solar energy is based on well-known heat transfer phenomena. In all thermal conversion processes, solar radiation is absorbed on the surface of a receiver, which contains or is in contact with flow passages through in which a working fluid pass.

I.1 Solar radiation:

Solar radiation reaches the Earth's surface in the form of direct solar radiation, diffuse solar radiation and reflected radiation, which can be overlooked. The total radiation received from the sun, from a horizontal surface to ground level for a serene day, is the sum of direct and diffuse radiation.

Direct radiation depends on the orientation of the receiving surface.

Diffuse radiation can be considered the same, regardless of the orientation of the receiving surface, although in reality there are small differences. Fig. 1 is the proportion of diffuse radiation in total I_G radiation [7].

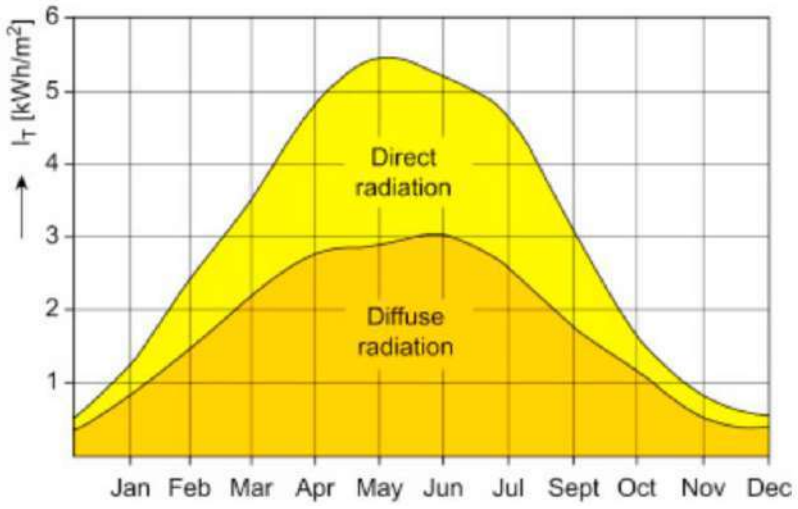

Figure I-1: Proportion of diffuse and direct radiation in total radiation I_G [7]

I.1.1 Direct solar radiation:

Direct solar radiation (I_G) is the proportion of almost straight solar radiation, which reaches the Earth's surface at an angle with a distance of 0.25° from the center of the sun and reaches a normal area, which is oriented perpendicular to the direction of radiation. The calculations in this study are based on the approach of Kasten (1989). Direct radiation is the part of the so-called extraterrestrial solar radiation (I_0), which reaches the Surface of the Earth directly after extinction in the atmosphere. I_0 depends on the actual distance (r) between the earth and the sun. Taking into account an average distance (r') [8], the average value of extraterrestrial radiation (solar constant I_0) is:

$$\boldsymbol{I'_0 = 1368\ W/m^2} \quad (1.1)$$

A correction of the distance (r/r) must be performed due to the slightly elliptical nature of the Earth's orbit. This applies to I_0 as follows:

$$\boldsymbol{I_0 = I'_0 (r'/r)^2} \quad (1.2)$$

According to astronomical formulas, we obtain the following formula for distance correction:

$$\boldsymbol{(r'/r)^2 = 1 + 0.03344 * \cos(x)} \quad (1.3)$$

$with\ x = 0.9856 * J - 2.72$;

J=Julian date=number of days, starting from 1=1 jan 12:00 UTC (global hour)

The Linke turbidity factor (T_{Linke}) is suitable for expressing the entire extinction, to which solar radiation is subjected in the atmosphere, because it indicates the optical density of a hazy and humid atmosphere compared to a pure and dry atmosphere.

T_{Linke} is the number of pure dry air masses that would cause the same extinction as the actual hazy and humid air examined [8]. Direct solar radiation ($_{DI}$) reaching the earth's surface can be parameterized as follows:

$$\boldsymbol{I_D = I_0\, exp(-T_{Linke} * D_{Ro} * m *\ p/p_0)} \quad (1.4)$$

With:

$\mathbf{I_D}$ = direct radiation in W/m2;

w/p_0 = 10 ((height above sea level)/18400*(1+0.004*T_A)); P0 = 1023.25 hPa;

T_A : air temperature in °C

D_{Ro}= vertical optical density of pure and dry standard atoms = D_{Ro}*m=1/(0,9+9,4/m);

m = relative optical air mass = 1/sin(h)

h = light angle ; sin(h)=sin(β)*sin(α)+cos(β)*cos(α)*cos(ξ)

α = geographical latitude of the place of observation;

β = declination of the sun = angle of the sun above the equator at the time of observation;

sin(β)=0.3978+sin[x-77.51+1.92*sin(x)];

ξ = hourly angle of the sun =(TLT-12h)*(15°/h);

TLT=true local time

I.1.2 Diffuse solar radiation:

Diffuse radiation is the part of solar radiation that arrives on the earth's surface after a single or repeated dispersion in the atmosphere. According to Valko, the intensity of diffuse radiation depends on 4 variables (Position of the sun, Rayleigh dispersion on clean air molecules, extinction by vapor particles, soil albedo) [8]

Due to the complexity of these physical processes and the difficulty of representing them by calculation, the measurement results often indicate substantial deviations from the calculated values. Valko's approach, which performs a multiple correlation based on the independent parameters of the solar angle, the Schuepp turbidity coefficient, the amount of cirrus, the number of clouds at the lower and middle levels as well as a seasonal coefficient, depending on the month [8]. The complete formula reads as follows:

$$\boldsymbol{I_d = C_j * (D_R + D_B)(KN_{LM} + KN_H - 1)} \quad (1.5)$$

with:

I_d = diffuse radiation in W/m2;

Cj = seasonal adjustment = 1+0.11*cos((J-15)2*π/365)); (Jendritzky, 1990)

J = number of days in the year (Julian date);

D_R= Scatter radiation by Raleigh dispersion in W/m2 = 39.78*sin(h)^0.35; (Jendritzky, 1990)

D_B= diffuse radiation by vapour dispersion in W/m2 = 2,6*sin(h)^0,66 *(10^3* B-12)^0,81

h = solar angle;

B = Schuepp turbidity coefficient;

K_{NLM} = low and medium cloud influence factor = 0.89 + 0.11 * 10 ^ ((0.17 * NLM));

N_{LM} = number of low- and medium-level clouds in tenths;

KN_H = cirrus influence factor = 1 + 0.035 * NH;

N_H = number of cirrus in tenths ;

I.1.3 Global solar radiation:

Solar energy or electromagnetic radiation that reaches the Earth's surface is partially absorbed on the surface, while the other part is reflected back to the atmosphere. The incoming light, apart from the component that comes directly from the Sun (this means that the light has not encountered any obstacles, the direction of direct radiation can be determined in each point of the Earth's surface), there is also a part of the light that refracts diffusely due to the particles in the atmosphere itself (for example, clouds, dust, smog and other aerosols), in this way, it changes the spectral distribution of the incident light. Apart from this, planet Earth itself emits electromagnetic radiation (Figure 2) [9].

The most common measurements of solar radiation are total radiation on a horizontal surface. [10]

$$I_G = I_D + I_d \tag{1.6}$$

$\boldsymbol{I_G} = global\ radiation\ in\ W/m2;$

$\boldsymbol{I_D} = direct\ radiation\ in\ W/m2;$

$\boldsymbol{I_d} = diffuse\ radiation\ in\ W/m2;$

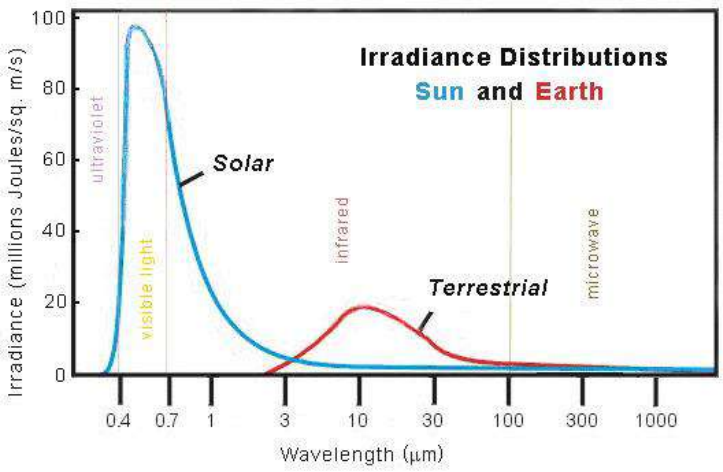

Figure I-2: Irradiation of the Sun and Earth [11].

I.2 Position parameters:

I.2.1 Geographical coordinates system:

The Earth's geographic coordinate system is the most common grid system used - the north and south poles are defined by the Earth's axis of rotation; equidistant between them is the equator. North-south latitude is measured in degrees from the equator, ranging from -90° at the south pole, 0° at the equator, to +90° at the north pole. East-west distances are also measured in degrees, but there is no "naturally defined" starting point – all longitudes are equivalent to all others. Humanity has arbitrarily defined the main meridian (0° longitude) as that of the Royal Observatory in Greenwich, England (alternately called the Greenwich meridian) [12].

Each degree (°) of a 360° circle can be subdivided into 60 equal minutes of arc ('), and each minute of arc can be divided into 60 seconds of arc ("). The Sommers-Bausch Observatory's 24-inch telescope is located at a latitude of 40°0'13" north of the equator and at a longitude of 105°15'45" west of the Greenwich meridian [12].

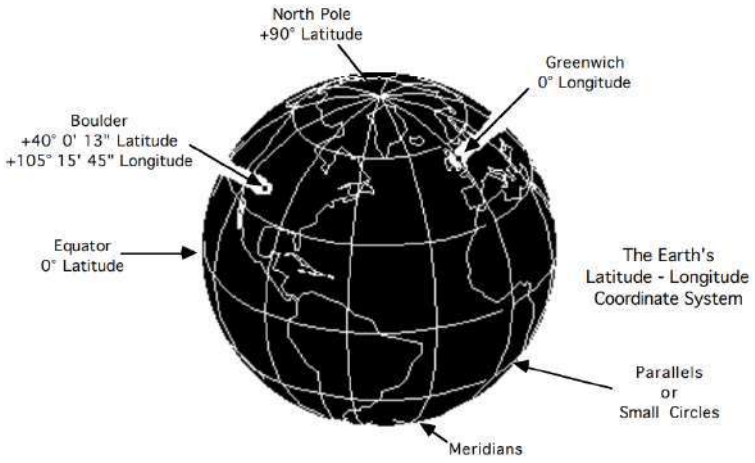

Figure I-3: The geographic coordinate system [12].

I.2.2 Horizontal Coordinate System:

The horizontal coordinate system is a celestial coordinate system that uses the observer's local horizon as a fundamental plane. It is expressed in terms of altitude angle (or elevation) and azimuth.

This coordinate system divides the sky into the upper hemisphere where objects are visible, and the lower hemisphere where objects cannot be seen since the Earth obstructs vision. The large circle separating the hemispheres is called the celestial horizon.[13]

The celestial horizon is a large circle on the celestial sphere with a plane that runs through the center of the Earth and is parallel to an observer's horizon. The pole of the upper hemisphere is called the zenith [13]. The pole of the lower hemisphere is called the nadir. There are two independent horizontal angular coordinates:

Altitude (E), or elevation, is the angle between the object and the observer's local horizon. The altitude is in the range [-90°, +90°] it is positive for objects above the horizon and negative for objects below the horizon. The zenith distance, or the angle between the object and the zenith, is:

$$z = 90° - \boldsymbol{E} \quad (1.7)$$

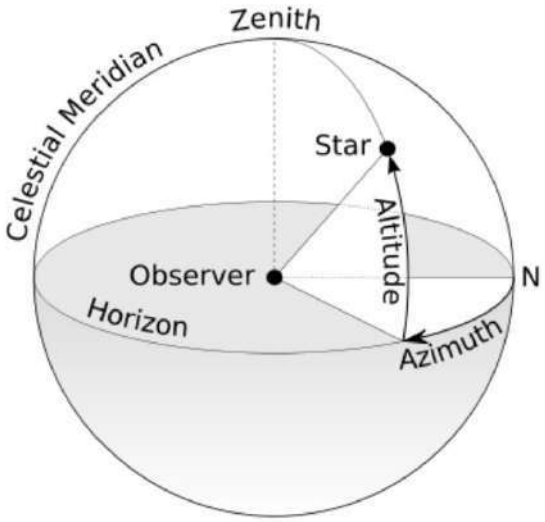

Figure I-4: Horizontal Coordinate System [13].

I.2.3 Equatorial Coordinate System:

This system is based on an extension of the Earth's axis of rotation, hence the name Equatorial Coordinate System. If we extend the Earth's outward axis into space, its intersection with the celestial sphere defines the north and south celestial poles; Equidistant from each other, and located directly above the Earth's equator, is the celestial equator.

The measurement of "celestial latitude" is called declination (DEC), but is otherwise identical to the measurement of latitude on Earth: the declination at the celestial equator is 0° and extends to ±90° at the celestial poles [12].

The east-west measurement is called right ascension (RA) rather than "celestial longitude", and differs from geographic longitude in two respects. First, the lines of longitude, or time circles, remain fixed in relation to the sky and do not rotate with the Earth. Second, the right ascension circle is divided into 24-hour time units rather than degrees; each hour of angle is equivalent to 15° of arc [12].

The following conversions are useful:

The Earth's equator is inclined by 23.5° relative to the plane of its orbital motion, or in terms of the celestial sphere, the ecliptic is inclined by 23.5° with respect to the celestial equator.

24 h = 360°	1 m = 15'
1 h = 15°	4 s = 1'
4 m = 1°	1 s = 15"

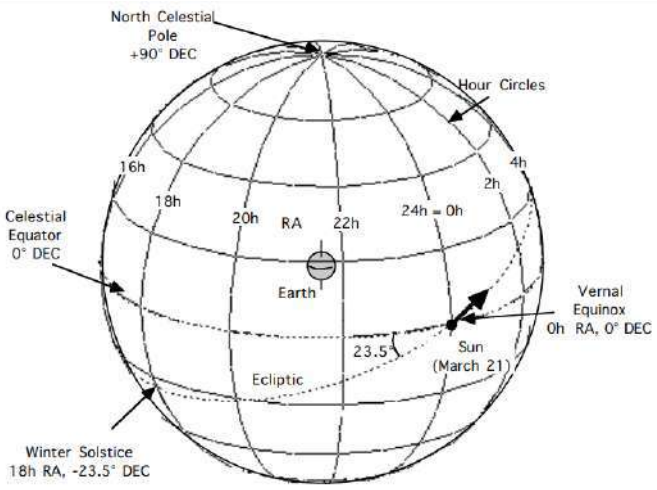

Figure I-5: Equatorial Coordinate System [12].

I.3 Solar deposit in Algeria:

Security threats, particularly in the south, combined with recent political changes and protests, can also pose real challenges. Yet Algeria's overall trajectory towards a cleaner and more sustainable energy sector is clear [14].

While the precise trajectory and timing of the sector's development will evolve over time, there is a clear momentum from the increasingly competitive economy of renewable energy technologies, growing consumer demand and Algeria's financial incentives to diversify its electricity sector [14].

In Algeria, the average annual sunshine is estimated at 3000 hours, with an average sunshine of 6.57 kWh / m2 / day. With 86% of the Saharan desert making up its territory and geographical position, Algeria has the largest solar field in the world. If we compare solar energy to natural gas, Algeria's solar potential is equivalent to a volume of 37,000 billion cubic meters per year, more than 8 times the country's natural gas reserves, with the additional difference that the solar potential is renewable, unlike natural gas [13].

I.3.1 Position parameters:

Algeria's geographical location has several advantages for intensive use of most RES (solar and wind). Algeria, located in central North Africa between 38°-35° north latitude and 8°-12° east longitude, has an area of 2381741 km2 and a population of 43.85 million (20.6 inhabitants/km2). Administratively, Algeria is divided into 48 provinces and lies, to the north, on the coast of the Mediterranean Sea. The length of the coastline is 2400 km. To the west, Algeria borders Morocco, Mauritania and Western Sahara, to the south-west of Mali, to the east of Tunisia and Libya and to the south-east of Niger (Figure 6) [3].

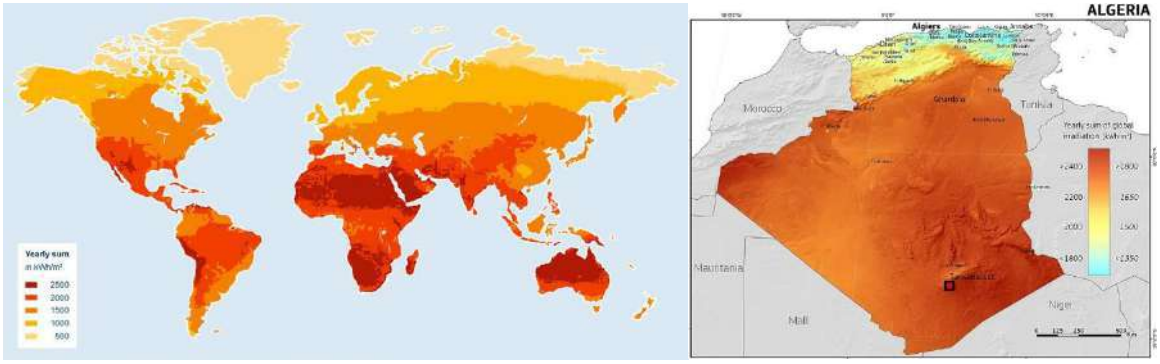

Figure I-6: Adapted solar sites located in the solar belt of the world and map of Algeria [3].

I.3.2 Average annual insolation and solar energy received:

The country receives an estimated direct irradiation of 169,440 kW/^{m2}/year with a potential production of 3000 kWh/year [2]. Table 1 shows the potential for solar energy production in Algeria. The country's desert is considered one of the areas where average solar irradiation and temperature are high in the world.

The duration of the insolation is about 2000 to 3900 h per year, with a horizontal surface radiation of about 3 to 5 kWh/^{m2}. There is a network of 78 weather measurement stations operated by the National Meteorological Office (ONM) throughout the country. Figures 7 and 8 show the distribution of irradiation and temperature in the country [2].

Location			
	Coastal area	**Inner area**	**Desert area**
Surface (%) **Average sunrise (hour/year)** **Average energy received (kWh/m2/year)**	**4** **2650** **1700**	**10** **3000** **1900**	**86** **3500** **2650**

Table I-3: Solar potential in Algeria [2].

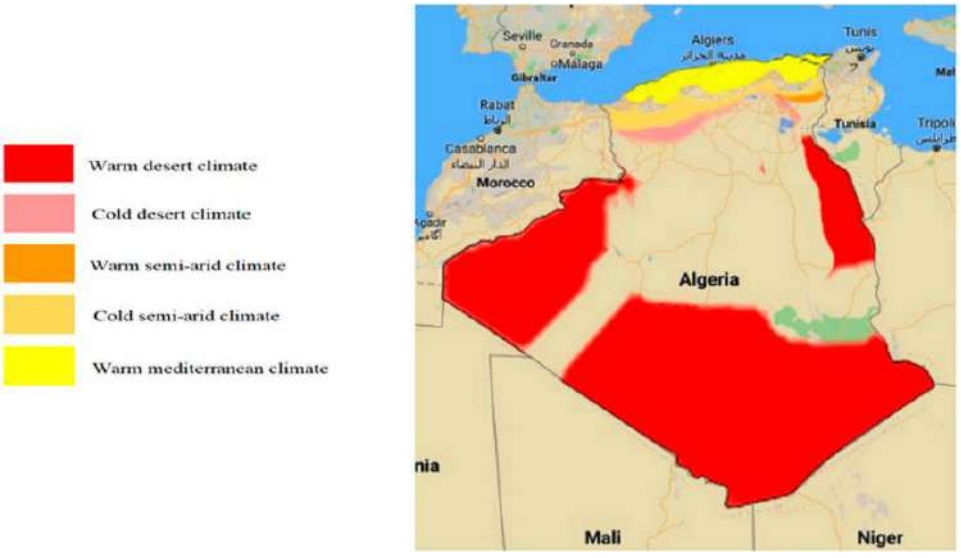

Figure I-8: The temperature distribution in Algeria.

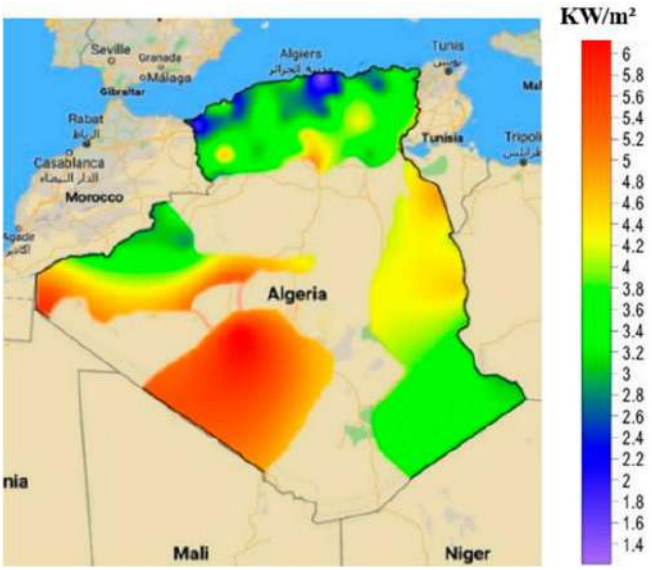

Figure I-7: Solar irradiation in Algeria kW/m^2 [3]

The desert area of the country covers 2048,297 km2 of land. This area has the potential to generate 168 × 1012 kWh/year through the use of 50% of the available space factor and an efficiency of 90% [3].

Ouargla is a good example, located in the Sahara Desert in southern Algeria (31.9527° N, 5.3335° E) with a total area of 2,887 km². It is a region with enormous solar potential, with solar radiation reaching 1600 W/m2 in summer, in addition to ambient temperatures of up to 45-50 C°, it is among the hottest regions on the planet which makes it a treasure trove of solar energy for the country of Algeria.

Chapter II

Different types of Solar collectors

Introduction:

Depending on the method of converting energy from solar radiation, solar recovery technologies can be divided into two main types: photovoltaic (PV) systems and solar thermal collectors. Photovoltaic panels generate electrical energy by absorbing solar energy via solar cells, which have an average efficiency of 15-17%. Solar power generation technology is widely used around the world. In the case of solar thermal collectors, solar energy directly heats a working fluid, which can collect heat in the solar collector for space and water heating. Conventional solar collectors have an average efficiency of 70%, but the efficiency varies depending on the type of solar collector [15].

II.1 Physical principles of the conversion of solar radiation into heat:

Solar energy can be used to produce refrigeration by converting solar heat into mechanical energy and using this power to drive a refrigeration machine. However, high collector temperatures are required to generate mechanical power with acceptable efficiency. Therefore, it is best to use a refrigeration machine.[16] An absorption refrigeration machine uses binary torque, for example (NH3-H20), the refrigerant is ammonia and the absorbent agent is water.

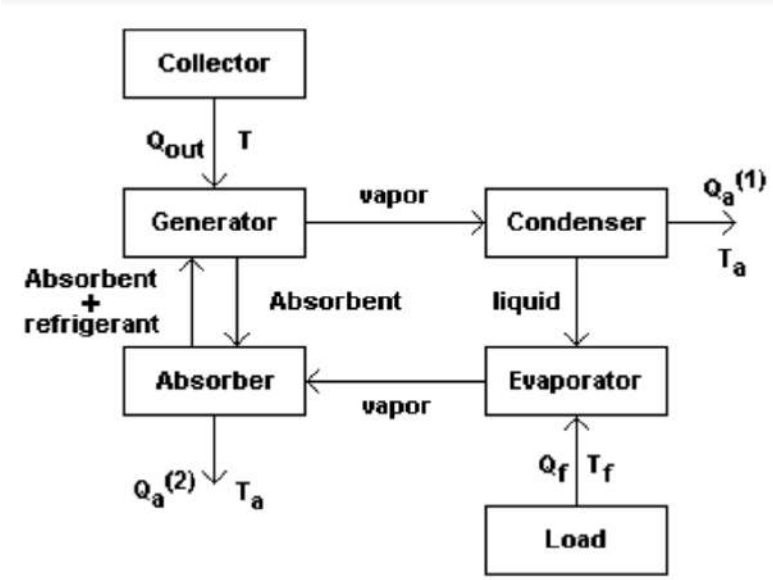

Figure II-1: Diagram of an absorption refrigeration machine [16].

II.2 Flat plate solar collectors:

Flat plate collectors are exploited to transform solar energy into useful heat mainly in the production of heated water for industry, residential and commercial applications [20].

II.2.1 Diagram of a Flat-plate collector:

Flat plate collectors consist of an absorbent plate, at the bottom of which pipes or tubes are installed. This is mounted in a hermetically sealed frame with a glass cover that is penetrable to solar radiation at the top and good thermal insulation at the bottom. Solar energy is absorbed by the black surface and provides heat to a fluid that flows through pipes or tubes. The heat is transferred to a process connected to the collector or stored [18].

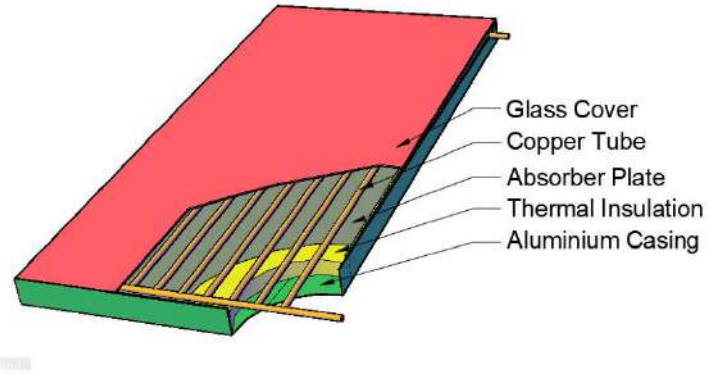

Figure II-2 : Diagram of a flat plate solar collector [19].

II.2.2 Principle of operation:

The absorbed radiation penetrates through the glass cover and hits the absorbent plate, transforming it into thermal energy. Excellent thermal conductivity is required since heat is transferred to the liquid, from the absorption plate to the absorbent tubes. With additional corrosion inhibitors used as heat transfer fluid, a water/glycol mixture is usually common in these applications.

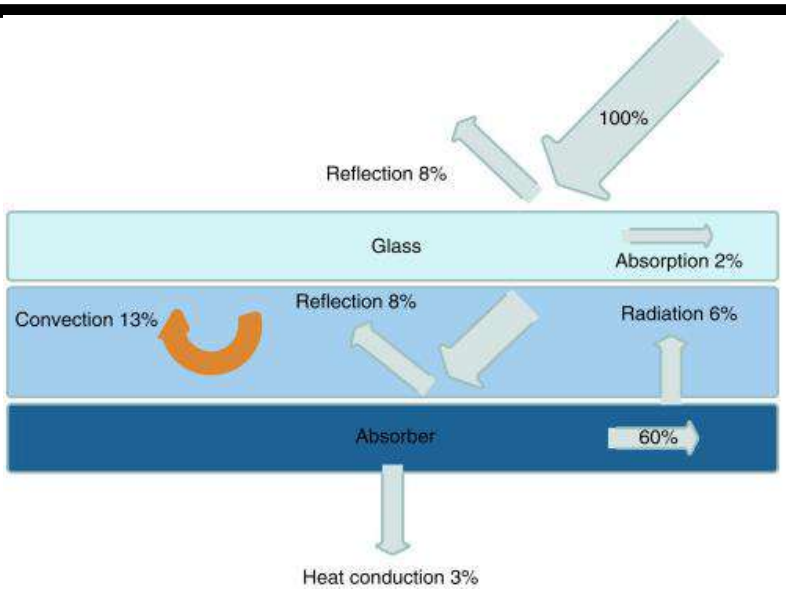

Figure II-3: Illustration of heat and optical losses in a flat plate collector [20].

II.2.3 Areas of use:

II.2.3.1 Water Heating Use Cases:

A closed-loop water heater using flat plate solar collectors is shown in Fig. II. 5 ; in this system, the water temperature is increased by flat plate solar collectors. To prevent water from freezing in winter, an antifreeze liquid is added and mixed with the water. The circulation pump will force water to flow through the heat exchanger (HEX). The high-temperature water from the flat plate collectors will exchange heat with the cold water supplied to the HEX, the cold domestic water will gain heat from the water heated by the flat plate collector and will be sent directly to users for use.[20]

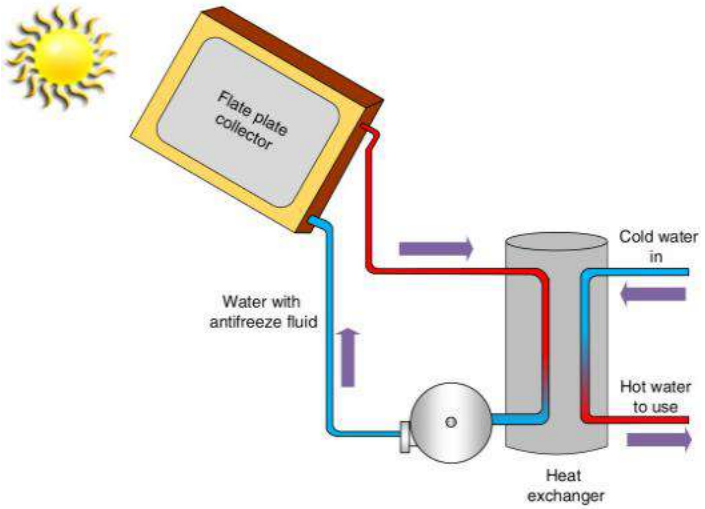

Figure II-4 : Diagram of a flat plate solar collector with a closed-loop water heater [20].

II.2.3.2 Space Heating Use Cases:

Active solar space heating systems (Fig. II. 6) use solar energy to heat an HTF (liquid or air) in a collector circuit, and then transfer the solar heat directly into the indoor space or into a storage tank for later use.

Liquid systems are more often used when storage is included and are well suited for radiant heating systems, boilers with hot water radiators and even absorption heat pumps. Thus, the distribution fluid (hot water) used by the existing heating system (e.g., radiator, radiant floor) flows through a heat exchanger into the storage tank. When hot water passes through the heat exchanger, it is heated and then returned to the heating system.[21]

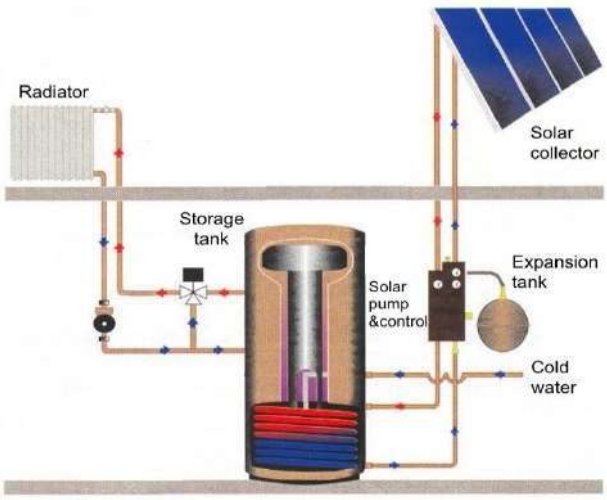

Figure II-5 : Diagram of an active solar heating system. [21].

Other uses of the flat solar collector include:

Solar cooling: In addition to heating applications, solar thermal systems can also meet cooling demands. In this case, solar thermal cooling systems can be used to replace gas or electric absorption/adsorption chillers or to replace electrically driven vapor compression air conditioning systems [22].

II.2.3 Advantages and disadvantages:

Advantages:

- Infinite source of energy.
- Easy to make.
- Pollution-free.
- Permanently fixed (no sophisticated positioning or tracking equipment is required).
- Less regional bias.
- Applications and various uses.

Disadvantages:

- Efficiency is usually low.
- Maximum temperatures cannot be reached due to the lack of optical concentration.
- The section from which heat is lost is important due to the lack of optical concentration.
- No power saving function for future use

II.3 Cylindrical-parabolic solar concentrators:

Solar concentrators are used to capture and focus the sun's rays to generate temperatures of up to 2000°C using mirrors and parabolic reflectors from a trough and dish system or refractive lens. This high-temperature heat is used to navigate chemical reactions [23].

II.3.1 Diagram of a Cylindrical-parabolic collector:

Parabolic trough systems, also known as linear hub systems, use U-shaped mirrors to concentrate most of the thermal energy they receive from the sun on a receiver; called a heat absorber or heat collector. The latter comes in the form of a long pipe located in the center, especially at the focal line of parabolic curvature reflectors.

It is filled with a heat transfer fluid, which retains heat well, such as synthetic oil or molten salt.[24]

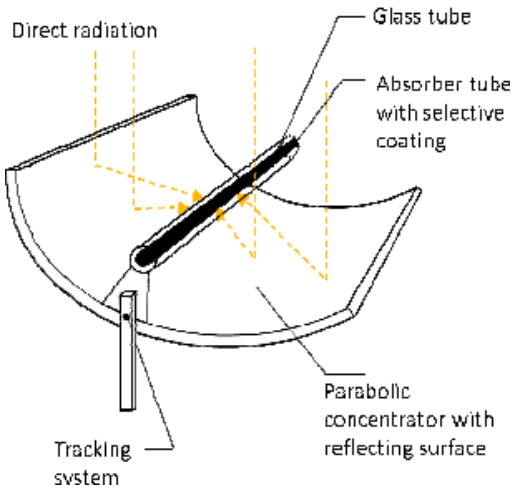

Figure II-6: Diagram of a parabolic trough concentrator [25].

II.3.2 Principle of operation:

The fluid absorbs heat from reflected solar radiation and becomes super-hot, reaching temperatures of about 390°C. It will then go through a heat exchanger to heat the water that circulates in it and transforms it into steam. The steam will turn into a standard steam turbine that will run a generator and produce electricity.[24]

After driving the turbine, the steam is recovered to be condensed and recycled again and again in the power generation systems. The same goes for the working fluid, which is also recycled and reused after transferring its heat into the water.

A typical solar collector field consists of several parallel rows of parabolic hollows aligned and oriented along a north-south axis to allow the east-west movement of the sun to be tracked during the day.[24]

This positioning increases the exposure time of the solar reflectors to solar radiation and ensures that the sun is continuously focused on the absorbent tube. The coatings on the latter make it possible to maximize the absorption of solar radiation and the use of a glass envelope evacuated around the pipe. Thus, it reduces heat loss to the environment.

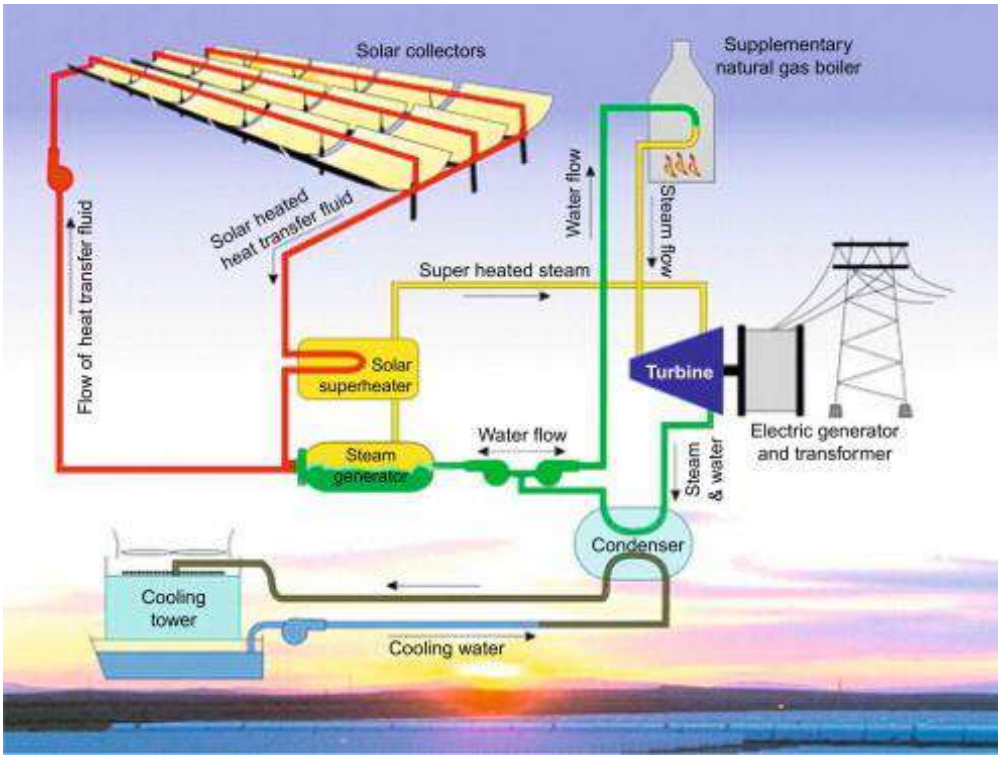

Figure II-7: A solar thermal system using parabolic collectors [26].

II.3.3 Areas of use:

II.3.3.1 Domestic hot water and space heating:

One of the most widespread applications of solar thermal energy is the production of hot water, both for ECS (kitchen, shower, laundry and sanitary facilities) and for space heating [27].

The temperatures at which the energy is required by these applications are below 100°C. Therefore, conventional solar collectors with appropriate yields could be used.

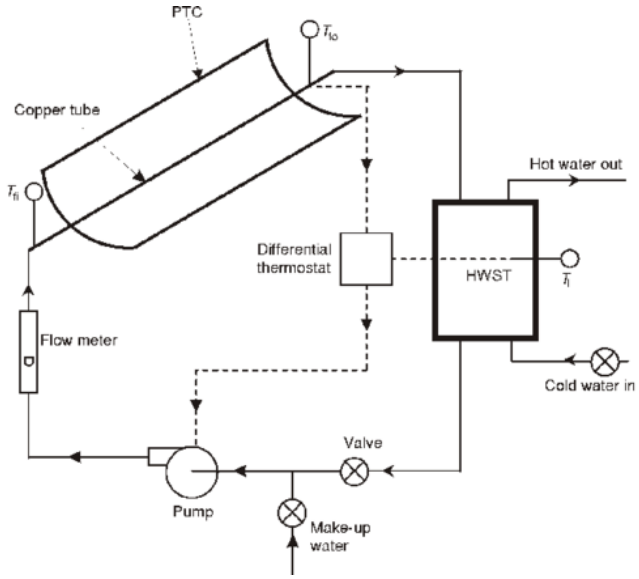

Figure II-8: Diagram of a parabolic trough water heating system [28].

II.3.3.2 Industrial process heat:

Industry is one of the world's largest energy consumers - about 30%. Key sectors are food and beverage, transport equipment, metal and plastic processing and chemicals. And the most suitable processes are cleaning, drying, evaporation and distillation, bleaching, cooking, melting [27].

The thermal energy demand for IPH (Industrial process heat) is less than 300 °C, and 37.2% of the total IPH demand is between 92 and 204 °C. According to the ECOHEATCOOL study carried out in 32 countries, 27% of the thermal energy demand for IPH is between 100 and 400 °C. For this reason, one of the most important applications of a small TPC is IPH [27].

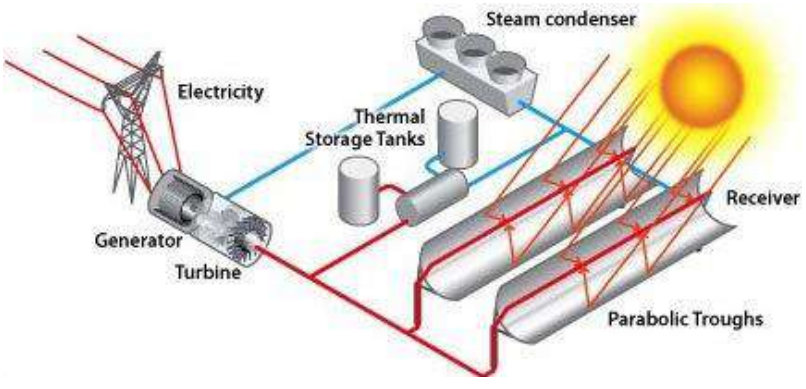

Figure II-9 : Standard Industrial Parabolic Trough Concentrator System [29].

II.3.3.3 Air conditioning and refrigeration:

The demand for energy associated with air conditioning in most industrialized countries has increased significantly in recent years, causing peaks in electricity consumption in hot weather and disrupting the transmission and distribution network. The main reasons for this growing demand for energy are the increase in heat loads, the improvement of the standard of living and comfort requirements of the occupants, as well as architectural features and trends, such as the increasing ratio between transparent and opaque areas in the building envelope [27].

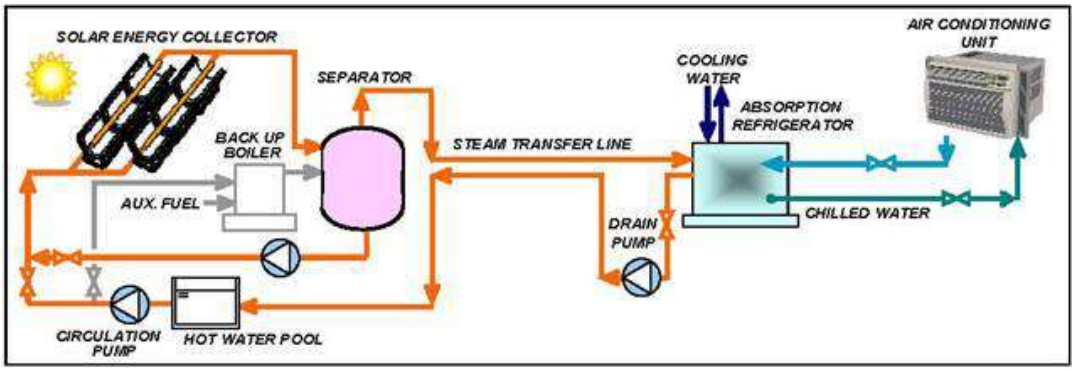

Figure II- 10: Solar-assisted air conditioning via a domestic heating network [30].

II.3.3.4 Desalination:

Solar desalination is one of the most promising technologies to address this problem because water scarcity and the availability of solar energy often coincide geographically [27].

Solar energy can be used for water desalination either directly, producing the distillates inside the solar collector, or indirectly, connecting the solar system to a conventional desalination plant.

In addition, the indirect concept can be realized with a solar thermal or photovoltaic system. While solar photovoltaic systems are used in electrical desalination plants, solar thermal systems can be connected to both a thermal and electrical desalination plant (by thermal-to-electrical intermediate conversion) [27].

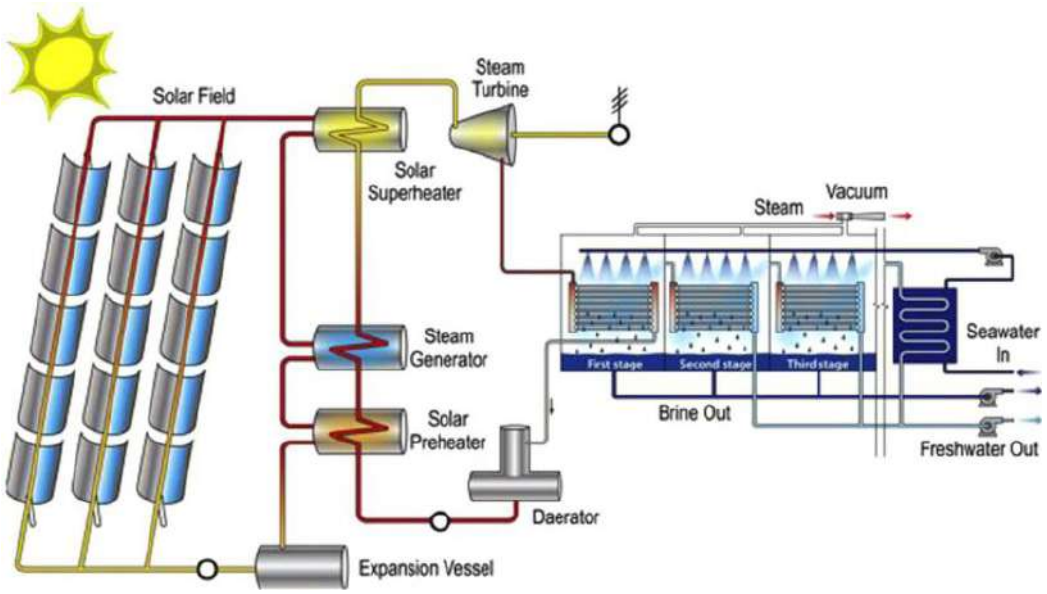

Figure II-11: Diagram of a solar-powered MED desalination plant [31].

II.3.4 Advantages and disadvantages:

Advantages:

- Increase in Intensity due to the concentration of energy over a large area on a smaller - area (receiver).
- Increased efficiency.
- Infinite source of energy.
- Reduced heat loss area due to optical concentration.
- The sophisticated alignment function ensures maximum use of solar energy.
- Delivery temperatures increase due to optical concentration (400°C -500°C).

Disadvantages:

- Higher cost.
- Additional equipment and maintenance are required.
- More dangerous (burns or eye damage).
- Increased complexity.
- More dependent on the direct beam.

Chapter III

Comparison between Flat-plate and Cylindrical-parabolic solar collectors

III. Introduction:

The overall production of a solar collector depends on the type of collector it is (non-concentrated or concentrated), how it is designed and the materials used to build its components.

The amount of energy that can be collected by a solar concentrator depends entirely on its position relative to the sun.

Flat plate collectors usually have limited temperature capacity and provide little or no concentration of indirect sunlight, so they work properly if left in a fixed position.

However, solar concentrators would collect so little energy in a fixed position that they must be equipped with the ability to track the sun daily from morning (east) to sunset (west) to be profitable.

Solar collectors installed in the southern parts of Algeria produce higher amounts of energy than those installed in the northern parts because the southern region is closer to the equator, meaning that the surface of this region receives a greater amount of sunlight and is exposed to an increased intensity of solar irradiation on a daily basis.

The objective of this chapter is to make a comparative study between the flat solar collector and the cylindrical-parabolic solar concentrator for the application of solar absorption refrigeration machine assisted solar air conditioning in Ouargla by evaluating the influence of various parameters on the efficiency of the two solar collectors

III.1 Energy balance and performance:

III.1.1 Flat plate solar collector:

Figure III-1 shows a schematic drawing of the heat flow through a collector. The question is how to measure its energy balance and thermal performance, i.e. the useful energy gain or the efficiency of the collector [35].

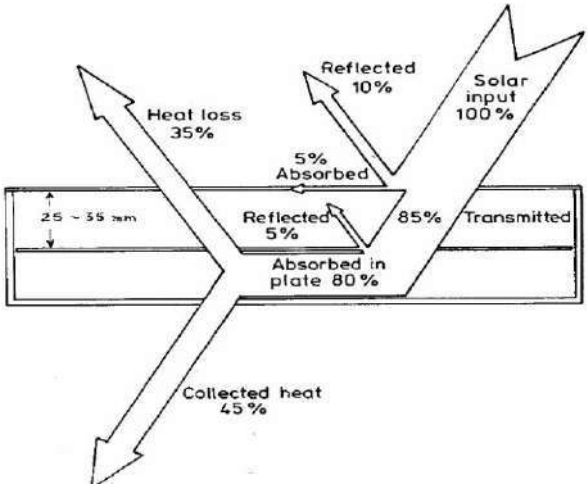

Figure III-1: Heat flow through a flat plate solar collector [35].

Figure III-2 shows the diagram of a typical solar system using a flat plate solar collector and a storage tank [35].

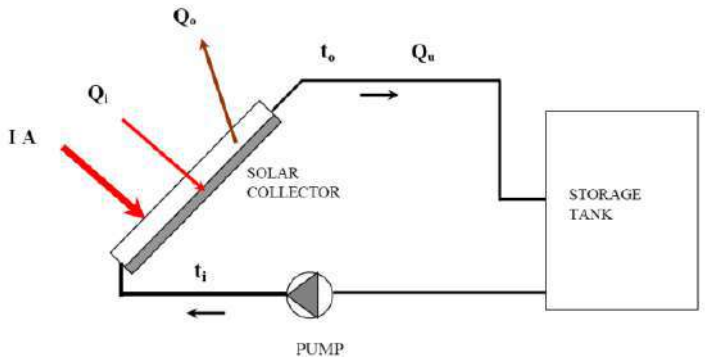

Figure III-2: Typical solar energy collection system [35].

If (I) is the intensity of solar radiation in W/m^2, incident on the opening plane of the solar collector having an area of (A), m^2, then the amount of solar radiation received by the collector is:

$$Qi = I * A \qquad (3.1)$$

However, as shown in Figure II-1, some of this radiation is reflected back to the sky, another component is absorbed by the glazing and the rest is transmitted through the glazing and reaches the absorbent plate in the form of short-wave radiation.
Therefore, the conversion factor indicates the percentage of sunlight entering the transparent cover of the collector (transmission) and the percentage absorbed.

$$Qi = I(\tau\alpha) * A \quad (3.2)$$

The heat loss rate (Q_0) depends on the overall heat transfer coefficient of the collector (U_L) and the temperature of the collector.

$$Q_O = U_L * A\,(Tc - Ta) \quad (3.3)$$

Thus, the rate of useful energy extracted by the collector (Qu), expressed as the rate of extraction under equilibrium conditions, is proportional to the rate of useful energy absorbed by the collector, minus the amount lost by the collector in its environment.

This is expressed as follows:

$$Q_U = Q_i - Q_O = AI\,\tau\alpha - U_L A\,(Tc - Ta) \quad (3.4)$$

Where τα is the transmittance absorption factor: $\tau\alpha = \frac{\tau_c \alpha_p}{1-(1-\alpha_p)*(1-\tau_c)}$ (3.5)

In addition, it is known that $Q_O = \dot{m} C_P (To - Ti)$ (3.6)

It is convenient to define a quantity that relates the actual useful energy gain of a collector to the useful gain if the entire surface of the collector was at the inlet temperature of the fluid. This amount is known as the collector heat removal factor (F_R) and is expressed as follows:

$$F_R = \frac{\dot{m}.C_P}{A_c.U_L}\left[1 - exp\left\{-\frac{F'.A_c.U_L}{\dot{m}.C_P}\right\}\right] \quad (3.7)$$

where F′ (collector efficiency factor) is given by: $F' = \frac{\frac{1}{U_L}}{W\left[\frac{1}{U_L[Do+(w-Do)F]}+\frac{1}{\pi Di.h_f}\right]}$ (3.8)

And F is the efficiency of the fins: $F = \frac{\tanh[m(W-Do)/2]}{m(W-Do)/2}$ (3.9)

Where $m = \sqrt{\frac{U_L}{\lambda_c e_p}}$ (3.10)

F_R can also be expressed as follows:

$$F_R = \frac{\dot{m}C_P(To - Ti)}{A[I\tau\alpha - U_L\,(Tc - Ta)]} \quad (3.11)$$

The maximum possible useful energy gain in a solar collector occurs when the entire collector is at the temperature of the input fluid. The real useful energy gain (Qu), Therefore, an energy balance equation n of the absorbing plate in the nominal form can be expressed for an equilibrium state condition as follows:

$$Q_U = F_R A[I\tau\alpha - U_L\,(Tc - Ta)] \quad (3.12)$$

A measure of the performance of a flat plate collector is the efficiency of the collector (η) defined as the ratio between the useful energy gain (Qu) and the incident solar energy over a given period of time:

$$\eta = \frac{\int Q_U\,dt}{A\int I\,dt} \quad (3.13)$$

$$\eta = \frac{Q_U}{AI} \quad (3.14)$$

Therefore, the instantaneous thermal efficiency of the collector is:

$$\eta = \frac{F_R A[I\tau\alpha - U_L\,(Ti - Ta)]}{AI} \quad (3.15)$$

$$\eta = F_R\,\tau\alpha - F_R U_L\,(\frac{Ti - Ta}{I}) \quad (3.16)$$

[35].

Application:

Consider a flat plate collector used to heat a thermal fluid with an inlet fluid temperature (Ti) of 40 – 90°C and a fixed flow rate of 0.1 kg / m^2s under these conditions that were encountered in the state of Ouargla (latitude 31.95 'N and longitude 5.33 'E) on May 18, 2022 at 11:00 am during the summer season:

Parameter	Value
Solar radiation (I)	1213 W/m^2
Ambient temperature (Ta)	33°C

Table III-1: Solar radiation (I) and Ambient temperature (Ta) in Ouargla, Algeria on May 18, 2022 at 1 1:00 a.m.

The following characteristics are available:

Specific heat of thermal fluid (Cpf): 2.3 kJ/kgK

Collector width (l): 0.89 m

Collector length (L): 1.95 m

Tube spacing (W): 120 mm.

Outer diameter of the tube (Do): 15 mm.

Inner diameter of the tube (Di): 13.5 mm.

Thickness of the absorbent plate (e_P): 0.4 mm.

Thermal absorption of absorbent plate (α_p): 0.906

Transmittance of the glass lid (τ_c): 0.95

Overall heat loss coefficient: 5.1 W/m^{2}K

Calculation:

$$\eta = F_R\,\tau\alpha - F_R U_L\,(\frac{Ti - Ta}{I}) \qquad (3.16)$$

If we assume that the heat removal factor F_R, Transmittance τ, Thermal absorption α and Overall heat loss coefficient U_L are constants for a collector and a given flow rate, then efficiency (η) is a linear function of the three parameters defining the operating conditions: solar irradiance (I), fluid inlet temperature (Ti) and ambient air temperature (Ta).

Calculation of constants:

$$F_R = \frac{\dot{m}.C_P}{A_c.U_L}\left[1 - exp\left\{\frac{F'.A_c.U_L}{\dot{m}.C_P}\right\}\right] \qquad (3.7)$$

$$F' = \frac{\frac{1}{U_L}}{W\left[\frac{1}{U_L[Do+(W-Do)F]}+\frac{1}{\pi Di.h_f}\right]} \qquad (3.8)$$

$$F = \frac{\tanh[m(W-Do)/2]}{m(W-Do)/2} \qquad (3.9)$$

$$m = \sqrt{\frac{U_L}{\lambda_c e_p}} = \sqrt{\frac{5.1}{385*0.0004}} = 5.75\text{m}^{-1} \qquad (3.10)$$

Therefore, $F = \frac{\tanh[5.75(0.12-0.015)/2]}{5.75\,(0.12-0.015)/2} = 0.97$

$$F' = \frac{\frac{1}{5.75}}{0.12\left[\frac{1}{5.1[0.015+(0.12-0.015)0.97]}+\frac{1}{\pi.0.0135.320}\right]} = 0{,}8273 \approx 0{,}83$$

$$F_R = \frac{\dot{m}.C_P}{A_C.U_L}\left[1 - exp\left\{-\frac{F'.A_C.U_L}{\dot{m}.C_P}\right\}\right] = \frac{0.1*2300}{(0.89*1.95)*5.1}\left[1 - exp\left\{-\frac{0.83*(0.89*1.95)*5.1}{0.1*2300}\right\}\right] = 0{,}8168 \approx 0{,}82$$

$$\tau\alpha = \frac{\tau_c \alpha_p}{1-(1-\alpha_p)*(1-\tau_c)} = \frac{0.95*0.906}{1-(1-0.906)*(1-0.95)} = 0.86 \qquad (3.5)$$

Thus, and $F_R\,\tau\alpha = 0.82 * 0.86 = 0.7052 \approx 0.70$ $F_R U_L = 0.82 * 5.1 = 4.182 \approx 4.1$

Now that we have obtained the values of each constant. The efficiency of the flat plate collector can be approximated using the three parameters (I, Ti and Ta) starting with Tin = 40 ° C, Ta = 30 ° C and *I* = 1213W / m2.

$$\eta = F_R\,\tau\alpha - F_R U_L \left(\frac{Ti - Ta}{I}\right) = 0.70 - 4.1\left(\frac{40 - 33}{1213}\right) = 0.6810 \approx 68.10\% \qquad (3.16)$$

The result is a single line (ΔT/I – Curve) shown in Figure III-3.

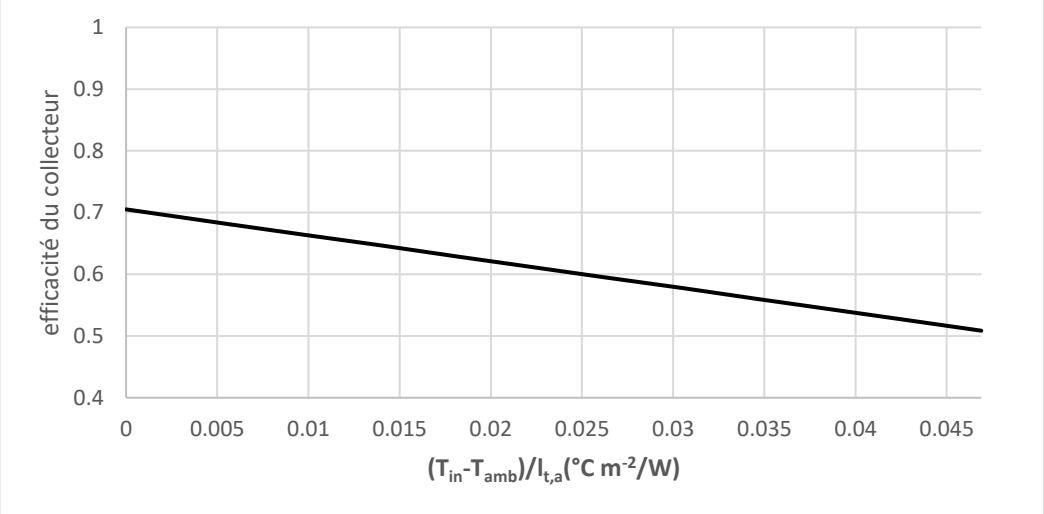

Figure III-3: Performance of a typical flat plate thermal collector

(T_a = 33 °C; I=1213W/m^2)

Interpretations:

Figure (III-3) shows the variation in the efficiency of a flat plate collector as a function of temperature difference (Ti – Ta)."

We notice a maximum efficiency of the collector of 70.52%, because the inlet temperature of the fluid is equal to the ambient temperature (Ti = Ta). Thus, the value ΔT/I is zero and the interception is FR (τ α). Then a gradual decrease in efficiency reaching as low as 50.86% at 90 ° C.

The entry at very high temperature caused a lower heat transfer which caused more heat loss, so the efficiency decreases under these kinds of conditions.

Therefore, the temperature change of the inlet fluid (Ti) is perpendicular to the percentage of efficiency, the higher Ti, the less efficient the collector.

III.1.2 Cylindrical-parabolic solar collector:

Figure III-4 shows the cross section of a typical solar system using a parabolic trough solar concentrator in use [36].

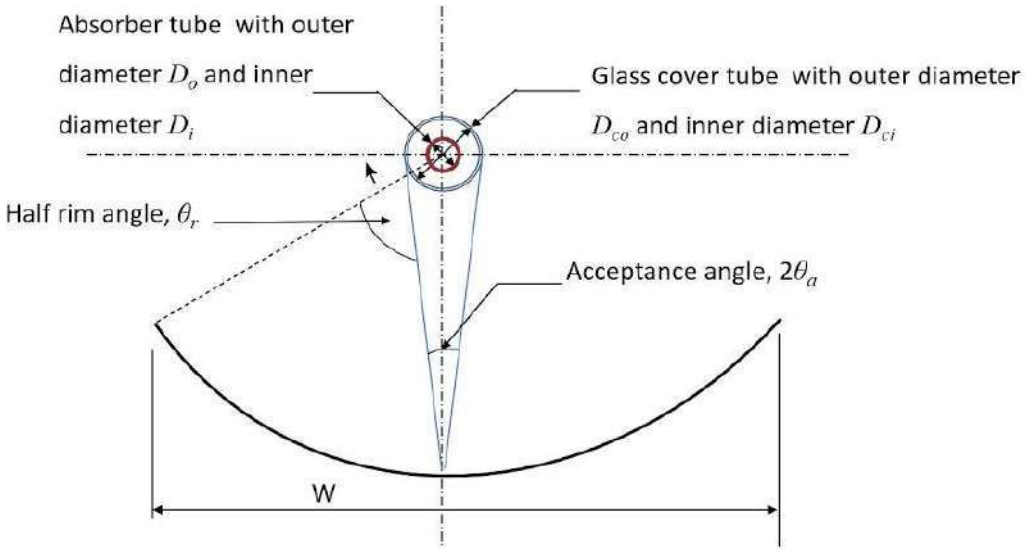

Figure III-4: Cross section of the cylindrical parabolic collector [33].

The energy balance of the solar collector and receiver helps us develop the optical and thermal analysis model to determine the performance of the collector.

Step-by-step performance estimation process:

1- With known values of diameters (Do, Di, Dco, Dci), length of the collector (L), mass flow of the fluid (ṁ) and inlet temperature of the fluid entering the collector (T_{fi}),

We can estimate the approximate value of the overall heat transfer coefficient:

$$UL = 4\ W/m2\ K$$

The mass flow rate of the fluid is given by: $$\dot{m} = \frac{\pi Di^2}{4} v_f \qquad (3.17)$$

2- now we can determine the speed of the fluid passing through the absorbent tube is:

$$v_f = \frac{\dot{m}4}{\pi Di^2} \qquad (3.18)$$

3- With known values of dynamic viscosity *(V)*, the Reynolds number (Re) can be calculated by:

$$Re = \frac{v_{f*}Di}{V} \quad (3.19)$$

With known values of Prandtl number (Pr) and thermal conductivity of the fluid (k_f), we can evaluate the heat transfer coefficient inside the absorber h_f:

Nu= 3.66 for Re <= 2000

Nu= $0.023*Re^{0.8}\,Pr^{0.4}$ for Re > 2000 (Pr is obtained from tables)

$$Nu = \frac{h_{f*}Di}{k_f} \quad (3.20)$$

4- collector efficiency factor $F' = \frac{1}{U_L\left[\frac{1}{U_L}+\frac{Do}{Di.h_f}\right]}$ *(3.21)*

5- heat loss factor of the collector $F_R = \frac{\dot{m}.C_P}{\pi.D_o.L.U_L}\left[1 - exp\left\{-\frac{F'.\pi.Do.L.U_L}{\dot{m}.C_P}\right\}\right]$ *(3.22)*

With the known values of collector width (W), specular reflectivity of concentrator surface (ρ), Mean value of transmittance absorption product (τα), Interception factor (γ), Incident solar radiation (I_b) Tilt factor (R_b), we can evaluate the absorbed flux S:

$$S = I\,R_b\rho\gamma(\tau\alpha) + I\,R_b(\tau\alpha)(\frac{D_o}{W-D_o}) \quad (3.23)$$

Where Rb is the tilt factor: $Rb = \frac{\cos\theta}{\cos\theta z}$ *(3.24)*

$$\cos\theta = \sin^2\delta + \cos^2\delta\cos\omega \quad ; \quad \cos\theta z = \sin\phi\sin\delta + \cos\phi\cos\delta\cos\omega \quad (3.25)$$

And τα is the transmittance absorption factor: $\tau\alpha = \frac{\tau_c\alpha_p}{1-(1-\alpha_p)*(1-\tau_c)}$ *(3.26)*

6- now we evaluate the rate of useful heat gain q_u with:

$$q_U = F_R(\mathrm{W} - Do)\mathrm{L}\left[S - \frac{U_L}{C}\{T_{fi} - T_a\}\right] \quad (3.27)$$

Where (C) is the concentration ratio $C = \frac{W-Do}{\pi.D_o}$ *(3.28)*

7- the rate of heat loss q_l is given by:

$$q_l = (W - Do)LS - q_U \quad (3.29)$$

8- q_L can also be expressed as:

$$q_l = \pi . Do . L . U_L (T_{pm} - T_a) \quad (3.30)$$

This expression is important because it is used to determine Tpm:

$$T_{pm} = T_a + \frac{q_l}{\pi . Do . L . U_L} \quad (3.31)$$

9- To evaluate the heat transfer coefficient between the absorbent tube and the cover h_{p-c}, we assume that the

Temperature of the collector Tc then:

$$T_m = T_a + \frac{T_{pm} + T_c}{2} \quad (3.32)$$

Now we can check the properties of the air at Tm

10- with T_{pm} known, we can evaluate the Rayleigh number:

$$R_a = g\beta\Delta T \frac{L_c}{V^2} = 9.81 * \frac{1}{T_{pm}} * (T_{pm} - T_c) \frac{L_c}{V^2} \quad (3.33)$$

The radial gap between the absorber and the glass cover L_C is given by:

$$L_c = \frac{D_{ci} - D_o}{2} \quad (3.34)$$

The modified Rayleigh number is given by:

$$(R_a')^{1/4} = \frac{\ln(D_{ci}/D_{co})}{{L_c}^{3/4} (\frac{1}{{D_o}^{3/5}} + \frac{1}{{D_{ci}}^{3/5}})^{5/4}} * {R_a}^{1/4} \quad (3.35)$$

11- now we can use the Raithby and Hollands relation to estimate the effective thermal conductivity:

$$\frac{K_{eff}}{K} = 0.317 (R_a')^{1/4} \quad (3.36)$$

Therefore, $$\frac{2K_{eff}}{\ln(D_{ci}/D_{ci})} (T_{pm} - T_c) = h_{p-c} \pi . D_o (T_{pm} - T_c) \quad (3.37)$$

Thus, the heat transfer coefficient plate to be covered is:

$$h_{p-c} = \frac{2K_{eff}}{D_o \ln(D_{co}/D_{ci})} \quad (3.38)$$

12- Using the Hilpert relation with the known value of the wind v∞, we can determine the heat transfer coefficient on the outer surface of the cover with:

$$Nu = C1Re^n \quad (3.39)$$

$$Re = \frac{v_\infty D_{ci}}{V} \quad (3.40)$$

Hilpert data for the new Reynolds number

Pour 40<Re<4000, C1=0,615, n=0,466

Pour 4000<Re<40 000, C1=0,174, n=0,618

Pour 40 000<Re<400 0000, C1=0,615, n=0,466

- check the properties of the air at Tm =(Tc-Ta)/2

$$h_w = \frac{N_u * k_{air}}{D_{co}} \quad (3.41)$$

13- The rate of heat loss per unit length from the absorber to the lid is given by:

$$\frac{q_{p-c}}{L} = h_{p-c}\left(T_{pm} - T_c\right) + \frac{\sigma\pi . D_o ({T_{pm}}^4 - {T_c}^4)}{\left[\frac{1}{\varepsilon_\rho} + \frac{D_o}{D_{ci}}\left(\frac{1}{\varepsilon_c} - 1\right)\right]} \text{ (W/m2)} \quad (3.42)$$

The rate of heat loss per unit length of the cover to ambient air is given by:

$$\frac{q_{c-a}}{L} = h_w(T_c - T_a) + \sigma\pi . D_o({T_c}^4 - {T_{sky}}^4) \text{ (W/m2)} \quad (3.43)$$

provided that we solve A and B to obtain the new Tc:

$$\frac{q_{p-c}}{L} = \frac{q_{c-a}}{L}$$

14- now we compare the new value of Tc with the hypothesis of step 9

If: assumed (Tc) - calculated (Tc) < ±1 is true, then we continue with the assumed value of Tc

Otherwise, we go back to step 9 and preform all the steps with a new value different from Tc

With the new value of Tc, we evaluate q_{p-c} / L then we obtain the new value of U_L

$$U_L = \frac{(\frac{qp-c}{L})}{L(T_{pm}-T_a)} \quad (3.44)$$

14- now we compare the new value of U_L with the hypothesis of step 1

If: assumed (U_L) - calculated (U_L) > ±1 is true, we return to step 1 and preform all steps with a new value different from U_L

Otherwise, we continue with the assumed value of U_L

15- finally we evaluate q_u, η and Tfo using:

$$q_U = F_R(\mathrm{W} - Do)\mathrm{L}\left[S - \frac{U_L}{C}\{T_{fi} - T_a\}\right] \quad (3.45)$$

$$T_{fo} = T_{fi} + \frac{F_R(\mathrm{W}-Do)\mathrm{L}\left[S-\frac{U_L}{C}\{T_{fi}-T_a\}\right]}{\dot{m}*\mathrm{Cp}} \quad (3.46)$$

$$\eta = \frac{F_R(\mathrm{W}-Do)\mathrm{L}\left[S-\frac{U_L}{C}\{T_{fi}-T_a\}\right]}{I_b R_b W L} \quad (3.47)$$

[33].

Application:

Consider a cylindrical-parabolic collector used to heat a thermal fluid that enters the receiver at a temperature of 60 °C with a flow rate of 0.4 kg/s. in these solar radiation conditions that were encountered in Ouargla (latitude 31.95'N and longitude 5.33'E), Algeria on May 18, 2022 from 6:00 am to 7:00 pm during the summer season. These values were obtained using the SOLPOS program of the NREL which uses Latitude, Longitude, time zone, surface pressure and ambient temperature of the dry bulb as input values.

Hour	6:00	7:00	8:00	9:00	10:00	11:00	12:00	13:00	14:00	15:00	16:00	17:00	18:00	19:00
Solar radiation (I_b) (W/m^2)	78	353	623	867	1069	1213	1291	1298	1232	1098	906	668	401	125

Table III-2: Solar radiation I in Ouargla, Algeria on May18, 2022 from 6:00 a.m. to 7:00 p.m.

The following characteristics are available:

Specific heat of thermal fluid (Cpf): 2.3 kJ/kgK

Location Ouargla, Algeria (φ, *I*): 31°95' N, 5°33'E

Date (n): May 18, 2022

Time: 6:00 a.m. - 7:00 p.m.

Ambient temperature (Ta): 33°C

Concentrator width (W): 2 m

Concentrator length (L): 6 m

Outer diameter of the absorber (D_o): 0.081 m

Inner diameter of the absorber (D_i): 0.075 m

Outer diameter of the glass envelope (D_{co}): 0.115 m

Inner diameter of the glass envelope (D_{ci}): 0.109 m

Interception factor (y): 0.94

Concentrator surface reflectivity (*p*): 0.86

Thermal absorption of the absorbent pipe (α_{ab}): 0.906

Thermal absorption of glass cover (α_g): 0.02

Transmittance of the glass cover (τ_g): 0.95

Overall heat loss coefficient (U_L): 6.7 W/m2k

Calculation:

$$\eta = \frac{F_R(\mathrm{W}-Do)\mathrm{L}\left[S-\frac{U_L}{C}\{T_{fi}-T_a\}\right]}{I_b R_b WL} \qquad (3.47)$$

$$S = I_b R_b \rho\gamma(\tau\alpha) + I_b R_b(\tau\alpha)\left(\frac{D_o}{W-D_o}\right) \qquad (3.23)$$

If we assume that the heat removal factor F_R, tilt factor R_b, concentration ratio C, transmittance τ, thermal absorptance α and overall heat loss coefficient U_L are constants for a given collector and flow, then efficiency (η) is a function of the four parameters defining the operating conditions: Absorbed flow (*S*), Solar irradiance (I_b), Fluid inlet temperature (T_{fi}) and Ambient air temperature (T_a).

Calculation of constants:

$$F_R = \frac{\dot{m}.C_P}{\pi.D_o.L.U_L}\left[1 - exp\left\{\frac{F'.\pi.Do.L.U_L}{\dot{m}.C_P}\right\}\right] \quad (3.22)$$

$$F' = \frac{1}{U_L\left[\frac{1}{U_L}+\frac{Do}{Di.h_f}\right]} = \frac{1}{6.7\left[\frac{1}{6.7}+\frac{8.1}{7.5*203}\right]} = 0.96 \quad (3.21)$$

$$F_R = \frac{\dot{m}.C_P}{\pi.D_o.L.U_L}\left[1 - exp\left\{\frac{F'.\pi.Do.L.U_L}{\dot{m}.C_P}\right\}\right] = \frac{0.4*2300}{\pi*0.081*6*6.7}\left[1 - exp\left\{\frac{0.96*\pi*0.081*6*6.7}{0.4*2300}\right\}\right]$$

F_R =0.9548 ≈ 0.95

$$C = \frac{W-Do}{\pi.D_o} = \frac{2-0.081}{\pi\times0.081} = 7.5411 \approx 7.54 \quad (3.28)$$

$$\tau\alpha = \frac{\tau_g\alpha_{ab}}{1-(1-\alpha_{ab})*(1-\tau_g)} = \frac{0.95*0.906}{1-(1-0.906)*(1-0.95)} = 0.86 \quad (3.26)$$

$$Rb = \frac{\cos\theta}{\cos\theta z} \quad (3.24)$$

Corresponding to the date and time of the given place (Ouargla (latitude 31.95'N and longitude 5.33'E), Algeria on May 18, 2022 at 11:00 am):

Latitude Φ = 31.9°

Angle of decline δ (138) = 19.43° (May 18: 138th day of the year)

Time angle ω (11hrs LAT) =-34.35°

From Eq. (3.25) :

$\cos\theta = \sin^2\delta + \cos^2\delta\cos\omega = \sin^2(19.43) + \cos^2(19.43)\cos(-34.35)$ =0.84

$\cos\theta z = \sin\phi\sin\delta + \cos\phi\cos\delta\cos\omega =$

$\cos\theta z = \sin(31.9)\sin(19.43) + \cos(31.9)\cos(19.43)\cos(-34.35) = 0.83$

$$Rb = \frac{\cos\theta}{\cos\theta z} = \frac{0.84}{0.83} = 1.012$$

Now that we have obtained the values of each constant. With fixed inlet fluid temperature (T_{fi}) and ambient temperature (T_a) values of 60°C and 33°C respectively, the performance of a cylindrical-parabolic collector can be approximated using solar irradiance (I_b) values over time from 78 W/^{m2} at 6:00 am.

$$S = I_b R_b \rho\gamma(\tau\alpha) + I_b R_b (\tau\alpha)\left(\frac{D_o}{W - D_o}\right) \quad (3.23)$$

$$S = 78 * 1.012 * 0.86 * 0.94 * (0.86) + 78 * 1.012(0.86)\left(\frac{8.1}{200 - 8.1}\right) = 57.74\ W/m2$$

$$\eta = \frac{F_R(\mathrm{W} - Do)\mathrm{L}\left[S - \frac{U_L}{C}\{T_{fi} - T_a\}\right]}{I_b R_b WL} \quad (3.47)$$

$$\eta = \frac{0.95 * (2 - 0.081) * 6\left[57.74 - \frac{6.7}{7.54}\{60 - 33\}\right]}{78 * 1.012 * 2 * 6} = 0.3892 \approx 38.92\%$$

The result is shown in Figure III-5.

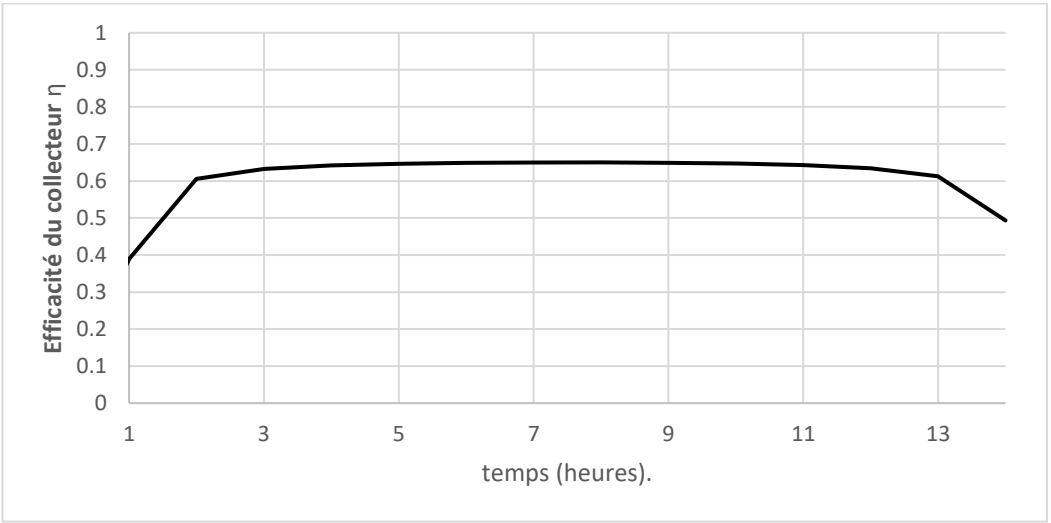

Figure III-5: Performance of a cylindrical-parabolic solar collector (T_{in} = 40°C T_a = 33°C).

Interpretations:

Figure (III-5) shows the change in the efficiency of a cylindrical-parabolic collector as a function of time (hours).

We notice a collection or efficiency of minimum of 38.92%, this is due to the low heat absorbed by the thermal fluid circulating through the absorbent tube caused by insufficient solar irradiance of only 78 W / m2 at 6:00 am (sunrise = insufficient sunshine).

Then a slow increase in efficiency reaching a maximum collector efficiency of 65.01% with solar radiation emitted from 1298 W/m2 at 13:00. (Noon = very adequate sunshine).

Efficiency begins to decrease to 49.36% with solar radiation of 125 W/m2 at 19:00. (Sunset = insufficient sunshine).

Therefore, the change in solar irradiance (I) is parallel to the percentage of efficiency, the higher I, the more efficient the collector.

III.2 Solar absorption refrigeration machine:

SARM (Solar Absorption Refrigeration Machine) are solar energy cooling systems that can meet both heating and cooling needs for home and industrial uses, they are very simple and can be used as economical air conditioning systems.

Although much research has been conducted on solar-absorbed air conditioning systems in order to make them economically and technically viable, there is still a lot of research in this area given their enormous energy potential, especially in a region with high average solar irradiation and high temperature like Ouargla, Algeria.

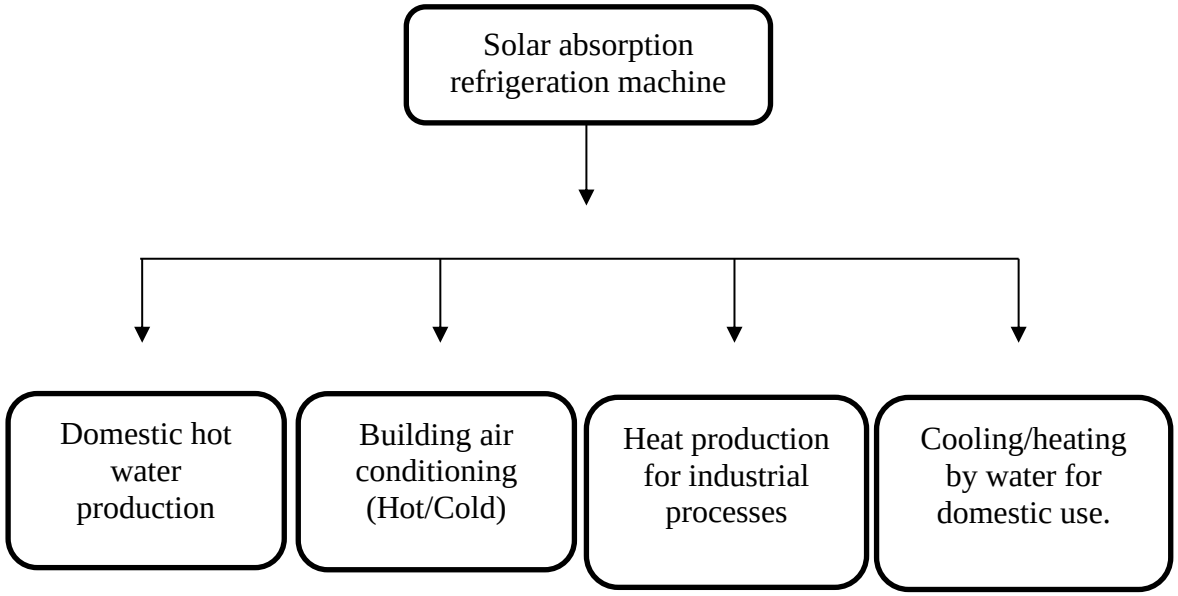

Figure III-6: Applications of solar-absorbed refrigeration systems.

III.2.1 Performance of a solar absorption refrigeration machine :

The performance of the refrigeration system is represented in the form of a "coefficient of performance (COP)". It shows how much heat can be removed from a cold region (Q_u) for each unit of energy used (Q_g).

$$COP = \frac{Qu}{Qg} \tag{3.48}$$

For solar-driven systems, performance can be written as the product of the COP and solar collector efficiency (η_c). In addition, it can be defined as a ratio between the refrigeration effect and the solar energy input for thermally driven systems, called the "thermal ratio of the system (STR):

$$STR = \frac{Qu}{I*A} = \frac{Qg}{I*A} * \frac{Qu}{Qg} = COP * \eta_{collector} \tag{3.49}$$

$$\eta_{system} = COP * \eta_{collector} \tag{3.50}$$

[35].

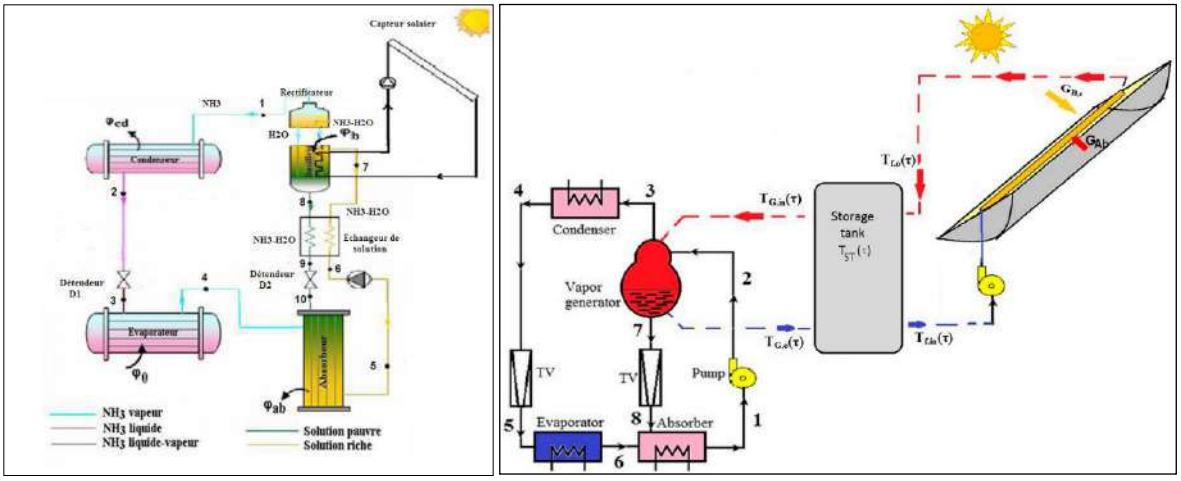

Figure III-7: Schematic diagram of MRSA powered by (a) FPC (b) CPC [34].

III.3 Parameters influencing the performance of solar collectors:

To make our comparison, consider two separate solar absorption refrigeration systems for use in a region of Ouargla aimed at providing water and air cooling during the summer season, one of these systems is coupled to a flat plate collector while the other to a cylindrical-parabolic collector.

III.3.1 Methodology:

We will study the influence of different parameters on the efficiency of solar collectors, one is a flat-plate collector while the other is a cylindrical -parabolic collector.

Flat plate collector	
Parameter	Value
Specific heat of the coolant (Cpf): Collector width (l): Tube spacing (W): Tube outer diameter (Do): Tube inner diameter (Di): Thickness of the absorbent plate (e_P): Thermal absorption of the absorbent plate (α_p): Transmittance of the glass lid (τ_c):	2.3 kJ/kgK 0.4 m 120 mm. 15 mm. 13.5 mm. 0.4 mm. 0.906 0.95

Table III-3: Fixed values of FPC to be used in the study.

Cylindrical-parabolic collector	
Parameter	Value
Specific heat of the coolant (Cp_f): Location Ouargla, Algeria (φ, *I*): Date (n): Hour: Hub width (W): Outer diameter of the absorber (Do): Inner diameter of the absorber (Di): Outer diameter of the glass lid (Dco): Glass lid of diameter (Dci): Interception factor (y): Concentration report: Tilt Factor Reflectivity of the concentrator surface (*p*): Thermal absorption of the absorbent pipe (α_{ab}): Thermal absorption of the glass lid (α_g): Absorbent tube glass lid transmission (τ_g):	2.3 kJ/kgK 31°95' N, 5°33'E May 20 2022 1100h 0.4 m 0.081 m 0.075 m 0.115 m 0.109 m 0.94 8.2 1.2 0.86 0.906 0.02 0.95

Table III-4: Fixed CPC values to be used in the study.

III.3.2 Results and discussion:

III.3.2.1 Effect of ambient temperature on performance:

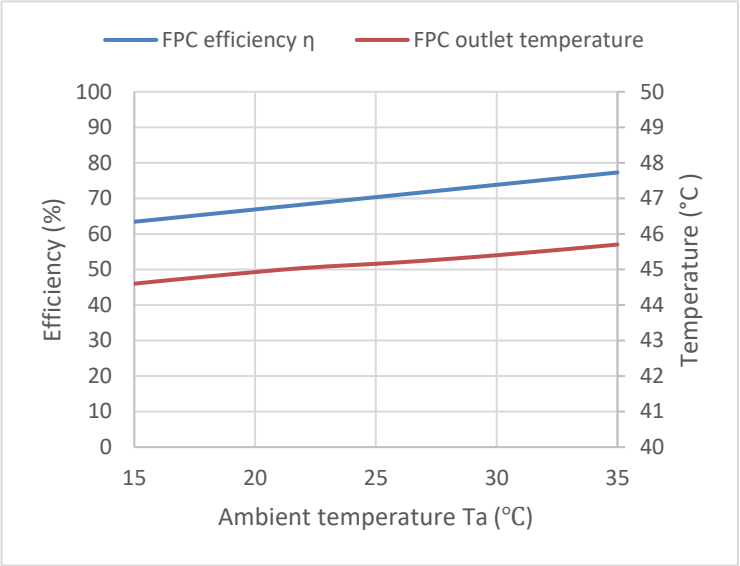

Figure III-8: Instantaneous FPC efficiency as a function of ambient temperature Ta (T_{in} = 40 °C; ṁ =0,4 kg/s; I = 850 W/m^2)

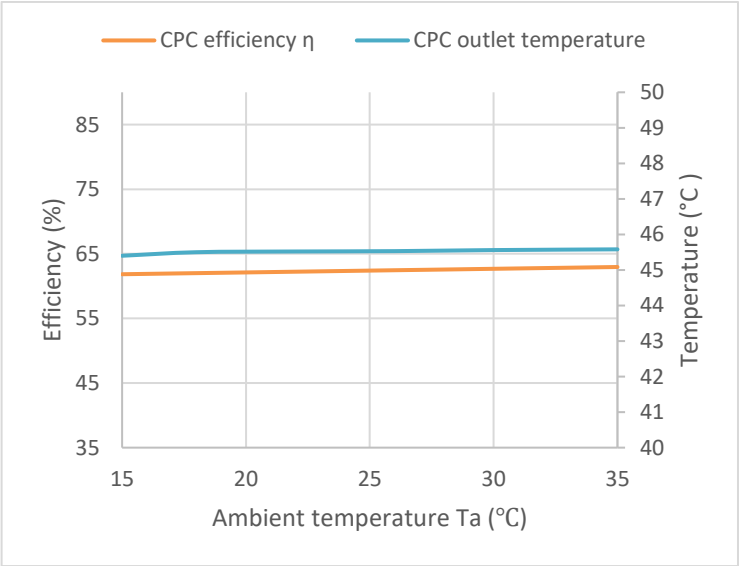

Figure III-9: Instantaneous CPC efficiency as a function of ambient temperature Ta (T_{in} = 40 °C; ṁ = 0,4 kg/s; I = 850 W/m^2)

Interpretations:

The two figures (III-8, III-9) show the change in instantaneous efficiency for FPC and CPC as a function of ambient temperature Ta.

The graph starts at a minimum efficiency at 15°C leading to a maximum efficiency at 35°C

As Ta increases, ΔT_{i-a} rises slightly with it, benefiting from the overall thermal efficiency of the collector due to the increased heat exchange between the glass cover, the absorber and the collector environment, which improves its efficiency under these conditions. Thus, the ambient temperature values and the temperature of the inlet coolant should be as close as possible for optimal performance.

III.3.2.2 Effect of solar irradiance on performance:

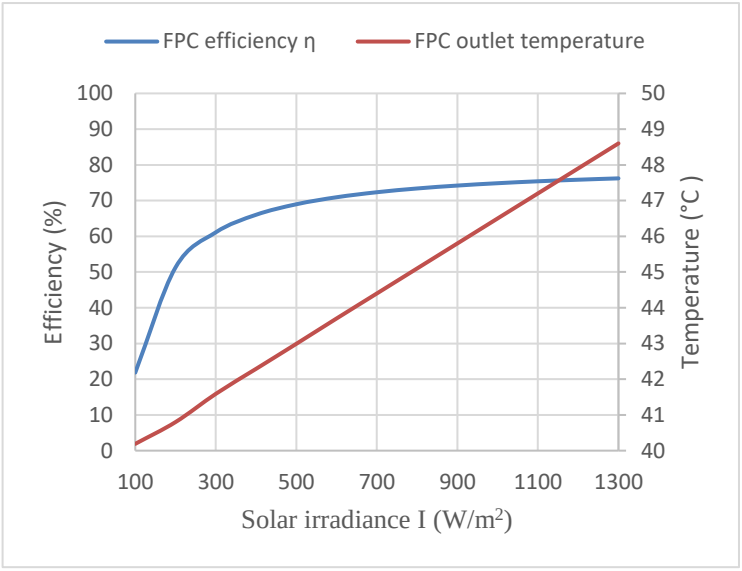

Figure III-10: Instantaneous FPC efficiency according to solar irradiance I.

(T_{in} = 40°C; T_a = 30 °C; ṁ =0,4 kg/s)

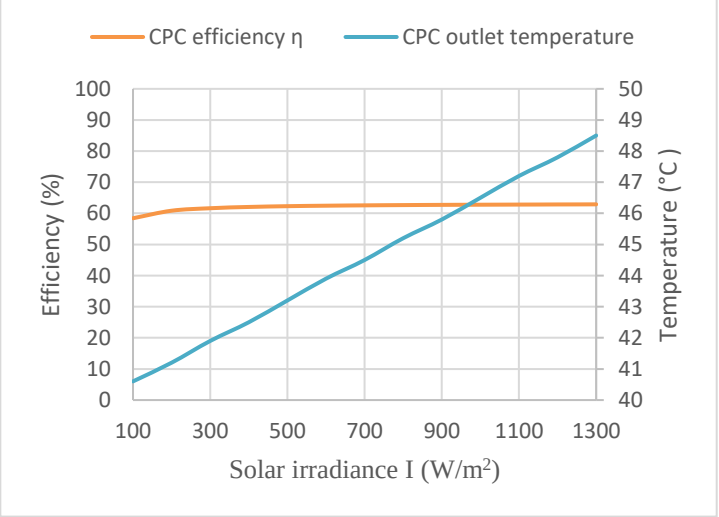

Figure III-11: Instantaneous efficiency of CPC according to solar irradiance I.

(T_{in} = 40 °C; T_a = 30 °C; ṁ =0,4 kg/s)

Interpretations:

The two figures (III-10, III-11) show the variation in instantaneous efficiency for FPC and CPC according to solar irradiance I.

We notice that the influence of solar irradiance is radically different between the two collectors, while it significantly increased the efficiency for FPC by (21-76%), it did not have much impact on the efficiency of CPC (58-62%).

This is because a cylindrical parabolic collector (CPC) accepts only one level of diffuse radiation on a moon-shaped segment of the hemisphere while an inclined FPC receives a level of diffuse radiation from the sky and a different level of diffuse radiation from the ground.

This problem is solved with concentration, we notice it at the beginning where at only 100 W / m2. CPC had a yield of 58%, while FPC had only 21%.

III.3.2.3 Effect of mass flow on performance:

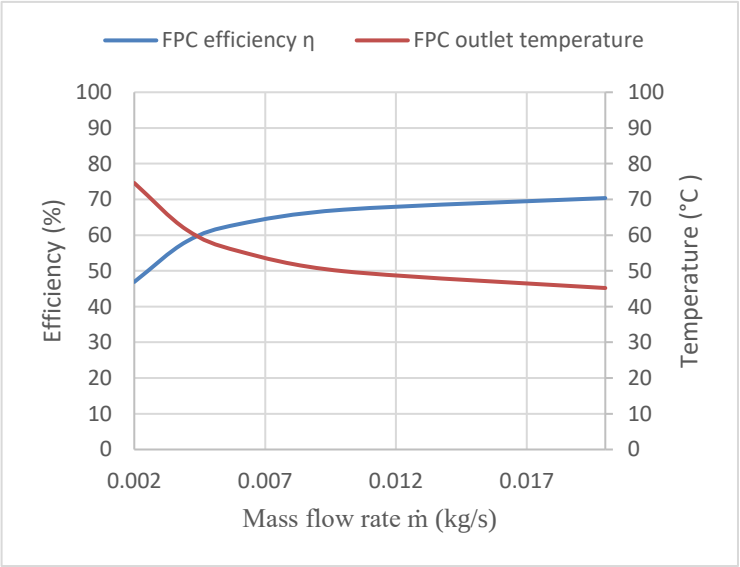

Figure III-12: Instantaneous FPC efficiency according to the mass flow rate ṁ.

(T_{in} = 40 °C;T_a = 40°C ; I = 850 W/m^2)

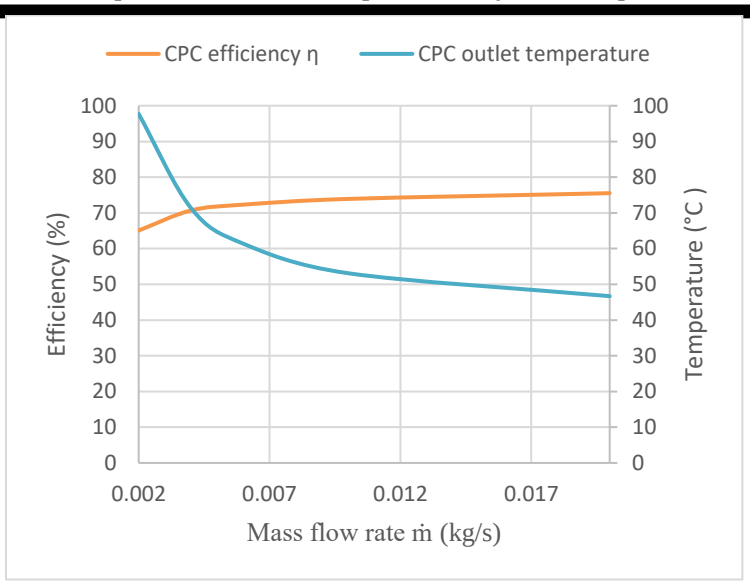

Figure III-13: Instantaneous CPC efficiency according to the mass flow rate ṁ.

(T_{in} = 40 °C; T_a = 40°C; I = 850 W/m^2)

Interpretations:

The two figures (III-12, III-13) show the evolution of the instantaneous efficiency for FPC and CPC as a function of the mass flow rate ṁ.

On notes that the mass flow rate ṁ has a nonlinear influence on the performance of the collector.

The nominal mass flow rate 0.006 kg/s is taken as a reference: 1/3 of its value, η decreased by 5%, x3 its value η is increased by 6%.

According to the figures (III-12, III-13), the value of the mass flow rate giving the best efficiency is the highest.

Increasing the mass flow rate of the working fluid improves convection heat transfer by intensifying the resistance to turbulence in the channel. In addition, thermal energy can be easily transferred now because the difference in mass flow between the cold and hot sides decreases the heat capacity ratio. Thus, increase the thermal efficiency of the collector. However, we also notice that the increase in mass flow has led to a considerable decrease in the coolant outlet temperature.

III.3.2.4 Effect of collector length on performance:

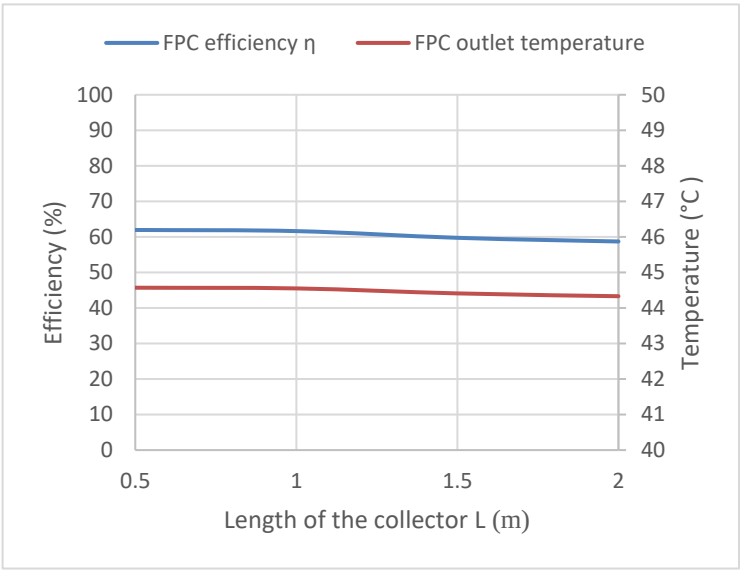

Figure III-14: instantaneous FPC efficiency according to the length of the collector L

(T_a = 30 °C ; ṁ = 0,4 kg/s; I = 850 W/m^2)

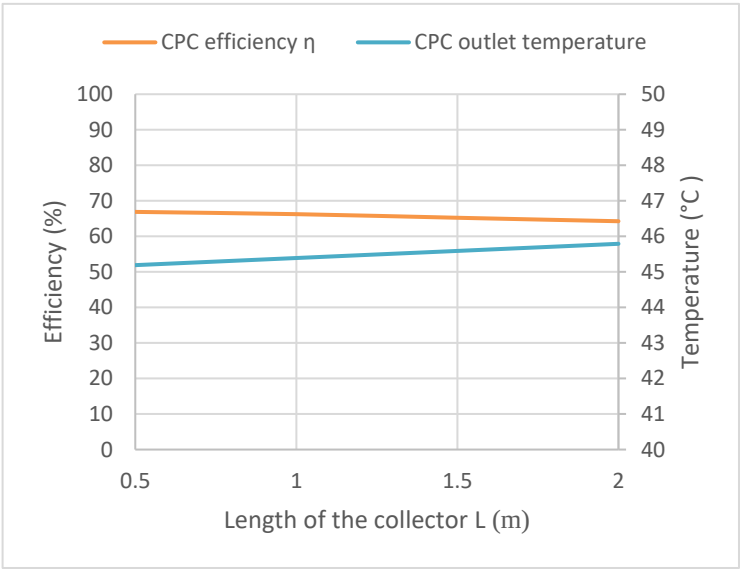

Figure III-15: instantaneous efficiency of the CPC according to the length of the collector L

(T_a = 30 °C ; ṁ = 0,4 kg/s; I = 850 W/m^2)

Interpretations:

The two figures (III-14, III-15) show the evolution of the instantaneous efficiency for FPC and CPC according to the length of the collector L.

Note that the length L of the collector has little or no influence on the performance of the FPC and CPC collectors (only 2% variation compared to L = 0.5 to 2 m)

This result is due to the linear dependence between L and ṁ: the mass flow is related to the surface of the collector, the change in length has no influence on the physical mechanism that occurs in the collector. Therefore, the length of the collector does not influence its performance.

III.3.2.5 Effect of absorbent plate thickness on FPC performance:

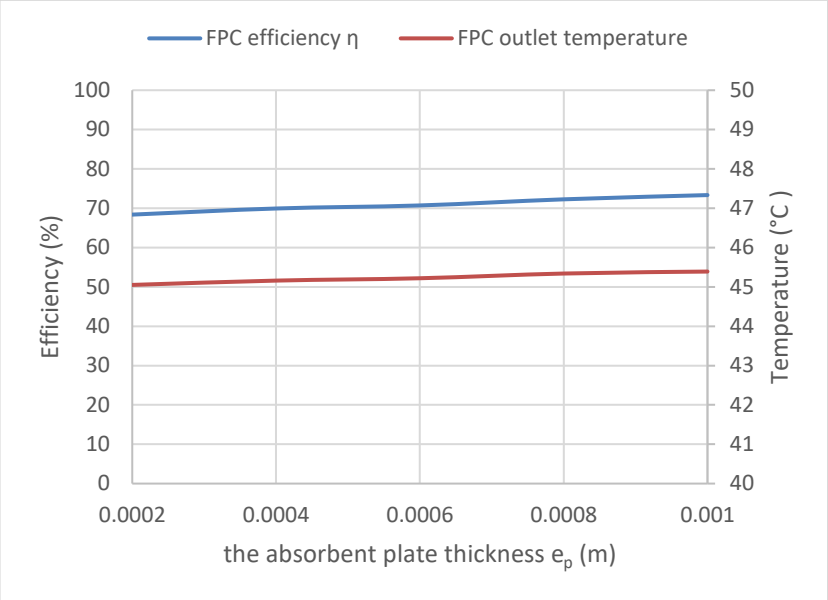

Figure III-16: Instantaneous FPC efficiency according to the absorbent plate thickness e_p. (Ta = 30 °C; ṁ = 0,4 kg/s; I = 850 W/m^2)

Interpretations:

Figure (III-16) shows the evolution of the instantaneous efficiency for FPC as a function of the thickness of the absorbent plate e_p.

We notice a slight increase in efficiency (change of about 5% from e = 0.0002 to 0.001 m)

This is because the thickness of the absorbent plate is related to the heat absorption performance. It must be chosen precisely to maximize thermal density and efficiency and not too large to minimize reverse efficiency and saturation current.

III.3.2.6 Effect of the tilt factor on CPC performance:

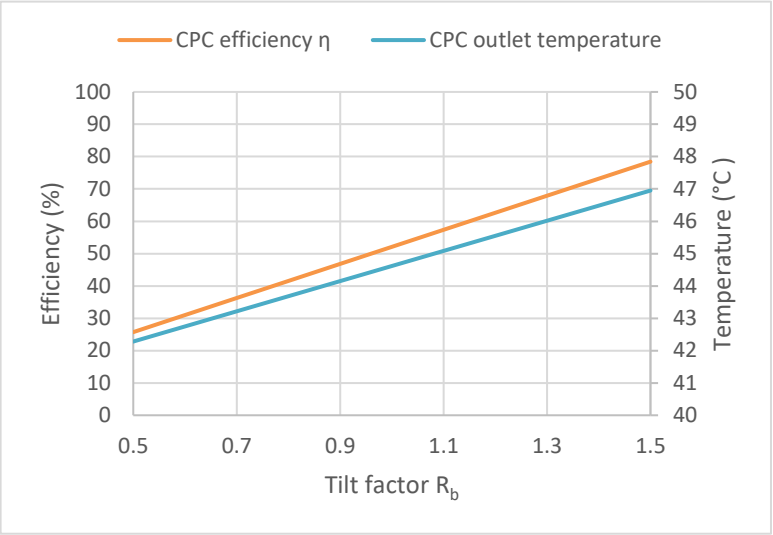

Figure III-17: instantaneous efficiency of CPC according to the tilt factor R_b

(T_a = 30 °C ; $\dot{m}$ = 0,4 kg/s; I = 850 W/m^2)

Interpretations:

Figure (III-17) shows the evolution of instantaneous efficiency for CPC according to the tilt factor R_b.

We notice that the tilt factor R_b has a significant influence on the efficiency of the collector (60% increase in R_b = 0.5 to 1.5).

This is due to the fact that the variation in the tilt factor completely changes the angle from which the collector surface receives sunlight and solar radiation reaching

The tilt factor R_b is used to set the tilt angle (tilt angle) and an orientation angle of the panel. The selection of these angles is done judiciously to achieve the maximum performance of the solar system when it operates without solar tracking over a specific period of time.

Conclusion:

We attempted to evaluate the influence of various parameters on the performance of the two collectors: flat-plate and cylindrical-parabolic solar collectors.

For parameters affecting the performance of FPC and CPC, the results show that increasing the length of a collector *L* has no effect on the performance of both collectors, increasing the mass flow *rate* $\dot{m}$ also improves the efficiency of both collectors, but the outlet temperature of the coolant T_{out} is then significantly reduced. Finally, incoming solar radiation *I* has a greater influence on the efficiency of the FPC compared to CPC, but results in roughly linearly the difference in output-input temperature. $\Delta_{out\text{-}in}$.

For parameters exclusive to FPC, the results show that increasing the thickness of the absorbent plate e_p has a small influence on the efficiency of the PFC.

For CPC-exclusive parameters, the results show that the increase in the tilt factor R_b significantly affected performance.

The incoming solar radiation I (increase of 10°C), the mass flow $\dot{m}$ (decrease of 30°C), the length of the collector L (increase of 100°C but only for the CPC), the tilt factor R_b (increase of 5°C).

General conclusion:

The country of Algeria, especially in the south, has huge solar potential due to its large area and geographical coordinates that place it at the forefront of many international solar projects, but security threats combined with political changes and protests pose real challenges and can delay Algeria's future towards a cleaner and more sustainable energy sector.

Solar energy can be used to produce refrigeration using solar thermal collectors, this is done by converting solar heat into mechanical energy and using this power to drive an absorption refrigerator that uses a refrigerant such as ammonia and an absorbent such as water.

Solar thermal collectors are distinguished by two types, non-concentrative or stationary (flat plate) and concentrating (cylindrical-parabolic). A non-concentrating collector uses a glass cover to intercept solar radiation and a metal plate to absorb its heat to transfer to a working fluid passing through copper tubes either for use (water or space heating) or for storage. While a sun-tracking concentration solar collector typically has concave reflective surfaces to intercept and concentrate radiation from the solar beam on an absorbent tube, thus further increasing the radiation flux, which is why these collectors are suitable for high-temperature applications such as industrial super-cooling and overheating processes, air conditioning and refrigeration.

Although flat plate collectors are simple, cost-effective and maintenance-free, they lack efficiency, do not save energy and can only be used for low-temperature applications. While cylindrical-parabolic collectors are more efficient, more sophisticated and achieve high temperatures, but they are due to higher cost, increased complexity, additional danger and dependence only on direct solar radiation.

Solar collectors best preform when installed with the right working conditions in mind, these conditions range from adjustments such as the use of high-quality insulation materials suitable for thermal application on fixed-position collectors to modifications such as the use of sun-tracking technologies on solar concentrators to ensure the lowest loss of solar radiation. and ensure the best possible performance. And finally, solar collectors installed in remote areas of the equator will not reach their full potential compared to those closer to them, this is due to the difference in climate, hours of sunshine and incoming solar irradiation on a daily basis.

The results show that the mass flow *rate* $\dot{m}$ and solar irradiation *I* are the most influential on the efficiency of the collector.

According to the results, the highest solar irradiation values *I* gave the highest efficiency for FPC and CPC. This is due to the high thermal conversion of the incident radiation inside the collector into useful thermal energy. We conclude the optimal value of solar irradiation *I* for this test at 1300 W/m^2 for FPC and CPC.

The results also showed that the highest mass flow values $\dot{m}$ gave the highest efficiency and the lowest heat losses for the FPC and CPC collectors, but this change in the mass flow rate $\dot{m}$ affected the outlet temperature of the coolant T_{out} negatively decreasing its value (97 ° C to 0.002 kg / s to 46 ° C to 0.02 kg / s for CPC and 74 ° C to 0.002 kg / s to 45 ° C to 0.02 kg / s for FPC), which is undesirable. We conclude that the optimal value of the mass flow *rate* $\dot{m}$ for this test is 0.004 kg/s for FPC and CPC.

The climate of Ouargla has continuously proven to be ideal for solar energy recovery and especially for solar thermal applications such as solar refrigeration and solar air conditioning, if these applications were indeed to be fully implemented, it could be extremely beneficial for the state of Ouargla economically and financially since the sun is an infinite and free source of energy.

With climate data from Ouargla during the summer season showing that the state receives solar radiation of up to 1200-1500 W/m^2, coupled with ambient temperatures reaching 40-50 °C, it is clear that cylindrical-parabolic collectors are the best option for air conditioning.

Despite their higher cost and increased complexity compared to flat-plate, cylindrical-parabolic collectors are not only much more efficient because of the sun-tracking option they are equipped with unlike flat plate collectors that remain in a fixed position, but because they concentrate the intercepted radiation on a smaller reception area, they get much higher delivery temperatures, reaching 2,50-400ºC compared to the flat plate with only 80-120°C.

Therefore, when it comes to a solar-rich region such as Ouargla, cylindrical-parabolic collectors are the logical option for high-temperature applications such as solar air conditioning, solar refrigeration, water processes for industrial heating as well as large-scale use such as food stores, buildings Apartments and water heating, while flat plate collectors are more suitable for low temperature applications such as domestic spaces and water heating, agricultural drying and solar cooking.

References

[1] **Zahraoui**, Y.; **Basir Khan**, M.R.; **AlHamrouni**, I.; **Mekhilef**, S.; **Ahmed**, M. Current Status, Scenario, and Prospective of Renewable Energy in Algeria: A Review. 14, 2354 Energies (2021)

[2] **A. B. Stambouli:** An overview of different energy sources in Algeria, Department of Electronics, Electrical and Electronics Engineering Faculty University of Sciences and Technology of Oran (2010)

[3] Energy & Mines, review of the energy and mining sector. N° 08, Nov. (2008)

[4] NOOR, Quarterly review of the Sonelgaz Group, n°10 - July (2010)

[5] **M.R. Alvarez** and **E. Zarza**, 'Concentrating Solar Thermal Power', Handbook of Energy Efficiency and Renewable Energy, (2004).

[6] **O. Ellabban, H.Abu-Rub, F.Blaabjerg ,** Renewable energy resources: Current status, future prospects and their enabling technology (2014).

[7] **Ioan Sarbu, Calin Sebarchievici** Solar Heating and Cooling Systems, (2017)

[8] **S. BECKER.** CALCULATION OF DIRECT SOLAR AND DIFFUSE RADIATION, Department of Geography, Justus-Liebig-Uniersity, Giessen, Germany. (2001).

[9] Vehbi Sofiu1 , Veis Šerifi. S.E.European University, Tetovo-Skopje, MACEDONIA (2011)

[10] John A. Duffie, William A. Beckman - Solar Engineering of Thermal Processes, Fourth Edition (2013)

[11] **Bjelopavlić, D.; Todorović, M**.: Solarni paneli, (2010).

[12] **U, Eiker**. Solar technologies for buildings, John Wiley sans Sons, England. (2001).

[13] **S.R.Ersoy, J.Terrapon-Pfaff** -Sustainable Transformation Of Algeria's Energy System, May (2021)

[14] **M.Hochberg**, Algeria charts a path for renewable energy sector development, (2020) https://www.mei.edu/publications/algeria-charts-path-renewable-energy-sector-development

[15] T.Boldoo , J.Ham , E.Kim, H.Cho. Review of the Photothermal Energy Conversion Performance of Nanofluids, Their Applications, and Recent Advances (2020)

[16] **R. H. B. Exell**, Principles of Solar Thermal Conversion - King Mongkut's University of Technology Thonburi (2000)

[17] **M.Fedkin** Overview of Solar Thermal Power Systems (2020).
https://www.e-education.psu.edu/eme811/node/682

[18] **V.Belessiotis, S.Kalogirou, E.Delyannis** Thermal Solar Desalination(2016).

[19] **Shamsul Azha, N.I.; Hussin, H.; Nasif, M.S.; Hussain, T**. Thermal Performance Enhancement in Flat Plate Solar Collector Solar Water Heater: A Review. Processes (2020)

[20] **Ibrahim Dincer, Muhammad F. Ezzat**, Comprehensive Energy Systems, 2018

[21] **Ioan Sarbu**. SOLAR WATER AND SPACE-HEATING SYSTEMS University of Timisoara, Romania (2018).

[22] IRENA Technology Brief R12- Solar Heating and Cooling for Residential Applications (2015)

[23] **Ashitha,S , Dr.Soney C. George**, Handbook of Biofuels, 2022

[24] **A,Berrada,R,El Mrabet**, Hybrid Energy System Models, 2021

[25] **Schiel, Wolfgang & Balz, Markus & Gabeler, Lena**. Glass – A material for concentrating solar energy plants. (2012)

[26] **Ziyad Salameh**, Renewable Energy System Design, 2014

[27] **A. Ferna´ndez-Garcı´a, E. Zarza, L. Valenzuela, M. Perez.** Parabolic trough solar collectors and their applications - (2010)

[28] **Arasu, A. & Sornakumar**, Theoretical analysis and experimental verification of parabolic trough solar collector with hot water generation system. (2007)

[29] **Salahuddin Qazi,** Standalone Photovoltaic Systems for Disaster Relief and Remote Areas (2017)

[30] Solar Trough Air Con/Pool Heating System (2011) https://sunearthenergy.wordpress.com/2011/01/05/solar-trough-air-conpool-heating-system-2/

[31] **Azevedo,** "Renewable Energy Powered Desalination Systems: Technologies and Market Analysis." (2014).

[32] **Fabio Struckmann** Analysis of a Flat-plate Solar Collector (2008)

[33] **S.E.M** Cylindrical Parabolic Collectors Optical and Thermal Analysis (2020) https://www.youtube.com/watch?v=-wIV8Mw0cuc&t=1463s.

[34] **C.Stanciu, D.Stanciu and A.Gheorghian** Thermal Analysis of a Solar Powered Absorption Cooling System (2017)

[35] **Mittal, V. & Kasana, Sanjay & Thakur, N. S.** The study of solar absorption air-conditioning systems (2005).

Appendices

Values set for the parameters studied:

Table III-4 - Values used in the study of ambient temperature (Ta).

Ta (°C)	*I(W/m2)*	*Tin* (°C)	F_R	U_L (W/m^{2}K)	τα	*L (m)*	*ṁ(kg/s)*
15	850	40	0.95	6.2	0.85	1	0.02
18	850	40	0.95	6.2	0.85	1	0.02
22	850	40	0.95	6.2	0.85	1	0.02
26	850	40	0.95	6.2	0.85	1	0.02
30	850	40	0.95	6.2	0.85	1	0.02
35	850	40	0.95	6.2	0.85	1	0.02

Table III-5 - Values used in the study of solar irradiance (I).

I(W/m2)	*Tin* (°C)	*Ta* (°C)	F_R	U_L (W/m^{2}K)	τα	*L (m)*	*ṁ(kg/s)*
300	40	30	0.95	6.2	0.85	1	0.02
400	40	30	0.95	6.2	0.85	1	0.02
500	40	30	0.95	6.2	0.85	1	0.02
600	40	30	0.95	6.2	0.85	1	0.02
700	40	30	0.95	6.2	0.85	1	0.02
800	40	30	0.95	6.2	0.85	1	0.02
900	40	30	0.95	6.2	0.85	1	0.02
1000	40	30	0.95	6.2	0.85	1	0.02
1100	40	30	0.95	6.2	0.85	1	0.02
1200	40	30	0.95	6.2	0.85	1	0.02

Table III-6 - Values used in the study of the mass flow rate (ṁ).

ṁ(kg/s)	*I(W/m2)*	*Tin* (°C)	*Ta* (°C)	F_R	U_L (W/m^{2}K)	τα	*L (m)*
0.002	850	40	30	0.95	6.2	0.85	1
0.004	850	40	30	0.95	6.2	0.85	1
0.006	850	40	30	0.95	6.2	0.85	1
0.01	850	40	30	0.95	6.2	0.85	1
0.02							

Table III-7 - Values used in the study of the length of the collector (L).

L (m)	*I(W/m2)*	*Tin* (°C)	*Ta* (°C)	F_R	U_L (W/m^{2}K)	τα		*ṁ(kg/s)*
0.5	850	40	30	0.95	6.2	0.85		0.02
1	850	40	30	0.95	6.2	0.85		0.02
1.5	850	40	30	0.95	6.2	0.85		0.02
2	850	40	30	0.95	6.2	0.85		0.02

Table III-8 - Values used in the study of the thickness of the absorbent plate (e_p) (FPC only)

e_p (m)	U_L (W/m^{2}K)	*I(W/m2)*	*Tin* (°C)	*Ta* (°C)	F_R	τα	*L (m)*	*ṁ(kg/s)*
0.0002	6.2	850	40	30	0.95	0.85	1	0.02
0.0004	6.2	850	40	30	0.95	0.85	1	0.02
0.0006	6.2	850	40	30	0.95	0.85	1	0.02
0.0008	6.2	850	40	30	0.95	0.85	1	0.02
0.001	6.2	850	40	30	0.95	0.85	1	0.02

Table III-9 - Values used in the study of the inclination factor (R_b) (CPC only)

R_b	U_L (W/m^{2}K)	*I(W/m2)*	*Tin* (°C)	*Ta* (°C)	F_R	τα	*L (m)*	*ṁ(kg/s)*
0.5	6.2	850	40	30	0.95	0.85	1	0.02
0.9	6.2	850	40	30	0.95	0.85	1	0.02
1.2	6.2	850	40	30	0.95	0.85	1	0.02
1.6	6.2	850	40	30	0.95	0.85	1	0.02
2	6.2	850	40	30	0.95	0.85	1	0.02

Abstract:

The country of Algeria particularly in the south has huge solar potential due to its large surface area and geographic coordinates putting at the front of many international solar projects, solar energy reaches the earth's surface as global radiation, this radiation consists of direct and diffuse solar radiation. we can harvest this radiation for the purpose of solar air conditioning with the aid of an absorption refrigerator using two solar collectors, non-concentrating or stationery (flat-plate) and concentrating (cylindrical-parabolic), a non-concentrating collector uses a glass cover for intercepting solar radiation and a metal plate for absorbing its heat to transfer it to a working fluid passing through copper tubes either for usage (water or space heating) or storage. whereas a sun-tracking concentrating solar collector usually has concave reflecting surfaces to intercept and focus the sun's beam radiation onto an absorber tube, thereby increasing the radiation flux even more. According to the study we did to further understand their performance, the mass flow rate $\dot{m}$ and solar irradiation I are the most influential on the efficiency of flat-plate and cylindrical-parabolic solar collectors. Our work concluded that cylindrical-parabolic solar collectors are the better option for high-temperature applications in the state of Ouargla such as air-conditioning and refrigeration, industrial super-cooling and super-heating processes, while flat plate collectors are more suitable for low temperature applications such as domestic spaces and water heating, agricultural drying and solar cooking.

تتمتع دولة الجزائر وخاصة في الجنوب بإمكانيات طاقة شمسية هائلة نظرا لمساحتها السطحية الكبيرة وإحداثياتها الجغرافية التي تضعها في مقدمة العديد من المشاريع الشمسية الدولية ، تصل الطاقة الشمسية إلى سطح الأرض كإشعاع شمسي- إجمالي ، ويتكون هذا الإشعاع من إشعاع شمسي- مباشر ومنتشر- ، يمكننا حصاد هذا الإشعاع لغرض تكييف الهواء بالطاقة الشمسية بمساعدة ثلاجة امتصاص باستخدام اثنين من مجمعات الطاقة الشمسية ، غير المركزة (لوحة مسطحة) والمركزة (أسطواني - مكافئ) ، يستخدم المجمع غير المركز غطاء زجاجيا لاعتراض الإشعاع الشمسي- ولوحة معدنية لامتصاص حرارته لنقله إلى سائل عمل يمر عبر أنابيب نحاسية إما للاستخدام (تسخين الماء أو الفضاء) أو التخزين. في حين أن المجمع الشمسي- المركز الذي يتتبع الشمس عادة ما يكون لديه الأسطح العاكسة المقعرة لاعتراض وتركيز إشعاع شعاع الشمس على أنبوب ممتص ، وبالتالي زيادة تدفق الإشعاع أكثر. وفقا للدراسة التي أجريناها لزيادة فهم أداء المجمعات الشمسية ، فإن معدل تدفق الكتلة $\dot{m}$ والإشعاع الشمسي- I هما الأكثر تأثيرا على كفاءة المجمعات الشمسية المسطحة والأسطوانية المكافئة. خلص عملنا إلى أن مجمعات الطاقة الشمسية الأسطوانية المكافئة هي الخيار الأفضل للتطبيقات ذات درجات الحرارة العالية في ولاية ورقلة مثل تكييف الهواء والتبريد الصناعي الفائق وعمليات التسخين الفائق، في حين أن المجمعات المسطحة أكثر ملاءمة لتطبيقات درجات الحرارة المنخفضة مثل تسخين المياه و المساحات المنزلية والتجفيف الزراعي والطهي بالطاقة الشمسية.